

A REVISED PROCEDURE FOR ANALYSIS OF INITIAL DATA
FOR A DYNAMICAL HURRICANE TRACK PREDICTION MODEL

by
Norma Jean Burrows Gordon
B.A., Colby College
(1973)

Submitted in partial fulfillment of the
requirements for the degree of
Master of Science
at the
Massachusetts Institute of Technology
June, 1977

Signature of Author.....
Department of Meteorology, May 12, 1977

Certified by.....
Thesis Supervisor

Accepted by.....
Chairman, Departmental Committee



A REVISED PROCEDURE FOR ANALYSIS OF INITIAL DATA
FOR A DYNAMICAL HURRICANE TRACK PREDICTION MODEL

by

Norma Jean Burrows Gordon

Submitted to the Department of Meteorology on
May 12, 1977 in partial fulfillment of the
requirements for the degree of
Master of Science.

ABSTRACT

The SANBAR hurricane track prediction model is a dynamical, barotropic model which relies on analysis of the wind field averaged through the depth of the troposphere. The current method of determining this initial flow pattern is discussed; and a revised procedure, which makes more and better use of the available data, is introduced for use in oceanic regions. It is expected that the new analysis method will generate a wind field which more closely approximates the mean tropospheric flow, thereby improving the SANBAR forecasts. Twenty-four cases from the 1975 hurricane season are rerun using the revised technique and are then compared with the operational forecasts. Contrary to expectation, no significant differences are observed, indicating that neither analysis procedure is superior. In some of the rerun forecasts, a deterioration of the initial analysis occurs poleward of 45°N latitude due to the lack of data in this region and to the elimination of bogus winds which are used in the operational runs. A bad analysis is also produced east of the storm in several reruns because of the strong reliance on upper-level winds. Overall, track directions are improved but forecast speeds are less in the rerun forecasts. Errors discovered in the stream-function and vorticity fields within the influence distance of the storm are partially responsible for the slowness observed in some of the selected cases. The revised forecasts are continuing to be examined to determine the reasons for the increased slow bias.

Thesis Supervisor: Frederick Sanders

Title: Professor of Meteorology

ACKNOWLEDGEMENTS

The author is grateful to Mark Zimmer of the National Hurricane Center for his cooperation in revising the SANBAR model and rerunning the selected cases, and to NHC and the National Center for Atmospheric Research (especially Paul Mulder) for providing essential data for this research. Special thanks go to Professor Frederick Sanders for his advice and guidance throughout the entire study. Thanks also go to Patricia Tayntor of MIT for data plotting and to Isabelle Kole for drafting the figures.

TABLE OF CONTENTS

	<u>Page</u>
List of Figures.....	5
List of Tables.....	7
Introduction.....	9
SANBAR Analysis Procedures in Oceanic Regions.....	11
Wind Analysis Within the Influence Distance of the Storm.....	13
A Revised Analysis Technique for Use in Oceanic Regions.....	16
Operational SANBAR Forecasts of 1975.....	20
Selection of Cases to be Rerun.....	29
Comparison of Errors for Selected Operational and Rerun Forecasts.....	30
Position Errors.....	30
Speed Errors.....	37
Direction Errors.....	41
Results of the Examination of the Rerun Forecasts...	43
Loss of the Stream-function Minimum.....	43
Analysis Poleward of 45°N.....	53
Excessive Weighting of 200-mb Level Winds.....	62
Errors in the Stream-function and Vorticity Fields Within the Area Influenced by the Storm.....	69
Conclusions.....	79
References.....	81
Appendix A.....	83
Appendix B.....	84

LIST OF FIGURES

<u>Figure</u>	<u>Page</u>
1. Map of SANBAR grid with bogus points and sample of computational grid.....	10
2. Map of unexplained variance in the analysis of the deviation of the zonal wind component from its zonal mean.....	19
3. Map showing areas in which the Eddy analysis continued to be performed and regions in which the new analysis procedure was carried out.....	21
4. Best tracks of 1975 storms.....	22
5. Sketch illustrating direction and speed errors..	26
6. Tracks of Faye, September 25, 1200GMT.....	47
7. Initial analyses of large-scale flow pattern, September 25, 1200GMT, for the operational and rerun SANBAR forecasts.....	50
8. Bogus winds and SANBAR grid point winds for the forecasts beginning September 25, 1200GMT.....	51
9. Tracks of Amy, July 1, 0000GMT.....	57
10. Initial analyses of large-scale flow pattern, July 1, 0000GMT, for the operational and rerun SANBAR forecasts.....	59
11. Bogus winds and SANBAR grid point winds for the forecasts beginning at 0000GMT on July 1.....	61
12. Tracks of Gladys, September 26, 1200GMT.....	65
13. Initial analyses of large-scale flow pattern, September 26, 1200GMT, for the operational and rerun SANBAR forecasts.....	67
14. Bogus winds and SANBAR grid point winds for the forecasts beginning at 1200GMT on September 26..	68

LIST OF FIGURES (CONT'D)

<u>Figure</u>	<u>Page</u>
15.Tracks of Gladys, September 28, 1200GMT.....	72
16.Initial analyses of large-scale flow pattern, September 28, 1200GMT, for the operational and rerun SANBAR forecasts.....	74
17.Bogus winds and SANBAR grid point winds for the forecasts beginning at 1200GMT on September 28..	75
B1.Correlation as a function of separation distance for departures of vertically-averaged wind from synoptic zonal average value.....	85

LIST OF TABLES

<u>Table</u>	<u>Page</u>
1. Regression equations for zonal and meridional components of mean tropospheric wind, based on rawinsonde observations at 850 mb and 200 mb....	14
2. Mean position errors for operational SANBAR forecasts.....	23
3. Mean magnitudes of speed and direction errors for operational SANBAR forecasts in 1975.....	27
4. Algebraic means of speed and direction errors for operational SANBAR forecasts in 1975.....	28
5. List of cases for revised forecasts.....	31
6. Mean position errors for selected operational forecasts.....	32
7. Mean position errors for rerun forecasts.....	33
8. Mean magnitudes of speed errors for selected operational forecasts and rerun forecasts.....	38
9. Algebraic means of speed errors for selected operational forecasts and rerun forecasts.....	39
10. Mean magnitudes of direction errors for selected operational forecasts and rerun forecasts.....	42
11. Algebraic means of direction errors for selected operational forecasts and rerun forecasts.....	44
12. Position errors for SANBAR forecasts for Faye, September 25, 1200GMT.....	46
13. Mean position errors for selected cases excluding cases in which the stream-function minimum was lost in one forecast and retained in the other.....	54

LIST OF TABLES (CONT'D)

<u>Table</u>	<u>Page</u>
14. Position errors for SANBAR forecasts for Amy, July 1, 0000GMT.....	56
15. Position errors for the SANBAR forecasts for Gladys, September 26, 1200GMT.....	64
16. Mean distances between operational and rerun SANBAR forecast positions for the selected cases.....	71
17. Position errors for SANBAR forecasts for Gladys, September 28, 1200GMT.....	70
18. Mean errors for the operational and rerun selected cases excluding forecasts with incor- rect vorticity values.....	78

INTRODUCTION

SANBAR is one of several hurricane prediction models used operationally at the National Hurricane Center (NEC) as guidance for official advisories on tropical storm and hurricane movement. Originally developed by Sanders and Burpee (1968), SANBAR is a dynamic, barotropic model which is based on the hypothesis that the track of a tropical cyclone is governed by the advection of vorticity in the mean tropospheric flow. The depth of the troposphere is taken as the layer from 1000 to 100 mb. The model utilizes winds from rawinsonde observations, representing the mean wind by a weighted average of the winds at the ten mandatory levels.

Obtaining an accurate initial large-scale flow field is difficult over oceanic portions of the SANBAR grid which are devoid of rawinsonde observations. Here, the model relies on 44 "bogus" winds at prescribed locations (see Figure 1). These winds are treated as genuine rawinsonde observations in the regression analysis used to obtain the SANBAR grid point winds. Wind estimates based on cloud-motion vectors obtained from geosynchronous satellites have become an important source of data for the analysis in oceanic regions. However, in the current method of analysis, much of this data enters into the model only indirectly. In this report, a revised analysis technique is introduced in which grid point winds are obtained without reference to the bogus points; satellite data, as

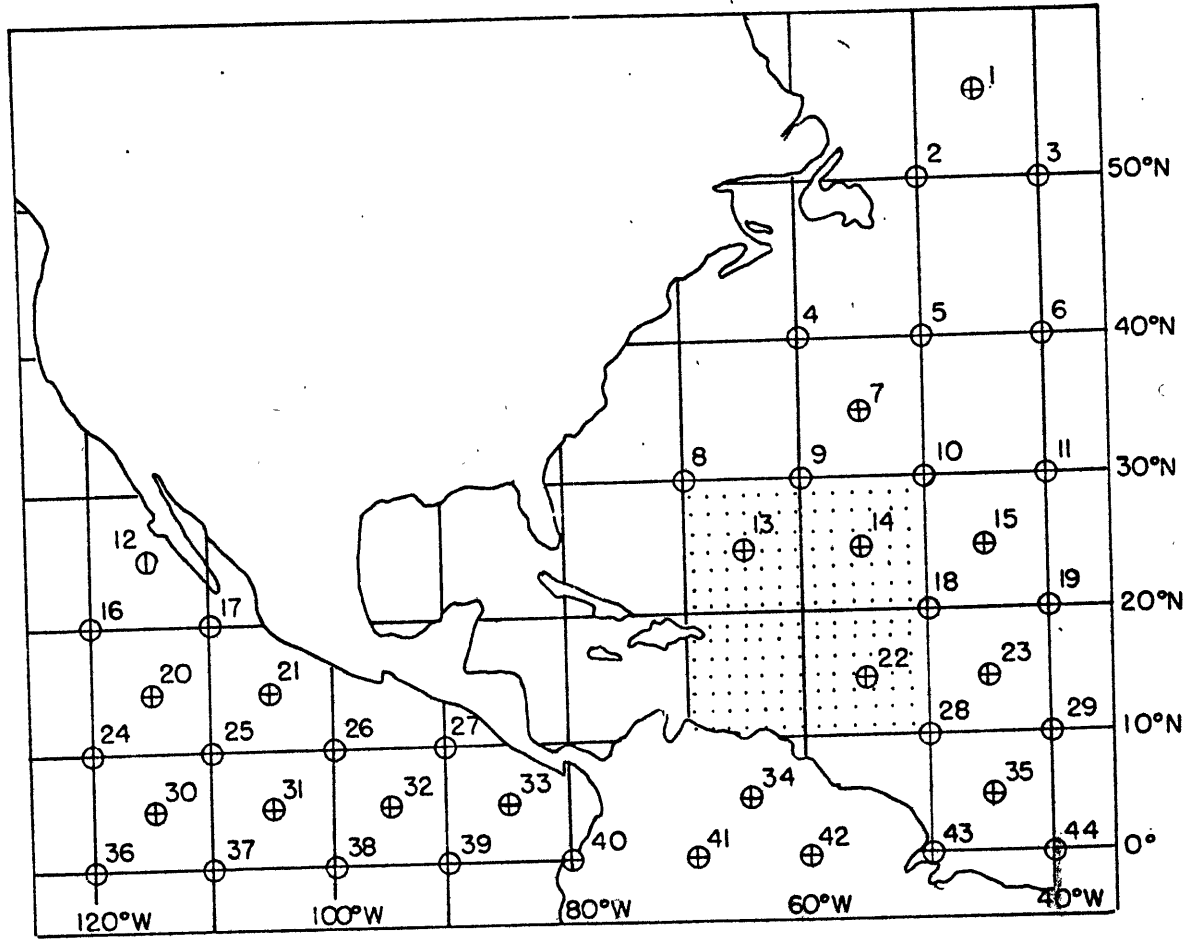


Figure 1. Map of SANBAR grid with bogus points and sample of computational grid.

well as ship and aircraft observations, enter into the program more directly. Selected cases from the 1975 hurricane season in the Atlantic Ocean were rerun at NHC using the new analysis procedure, and the results are compared with the operational SANBAR forecasts.

SANBAR ANALYSIS PROCEDURES IN OCEANIC REGIONS

Originally, the mean winds at the bogus points were determined subjectively by consideration of the 500-mb analyses prepared by the National Meteorological Center (NMC), the surface and 200-mb analyses prepared manually at NHC, and any available reconnaissance aircraft wind information. This procedure was time consuming and often the analyses used were 12 hours old. These problems were remedied by the automation of the analysis of the flow at the ATOLL (Analyses of the Tropical Ocean Lower Layer) and 200-mb levels at NHC (Wise and Simpson, 1971) and the automation of bogus point estimation (Pike, 1972b).

Currently, an elliptical scanning technique is used to determine the zonal and meridional components of the wind at each grid point at the ATOLL and 200-mb levels (Wise and Simpson, 1971).¹ The analysis procedure involves the application of corrections to a "first guess" field and is similar to that developed by Cressman (1959). This scanning procedure is described in Appendix A.

¹The analysis was originally performed on an NHC grid which had a 90 n mi mesh length.

The NMC 850- and 200-mb analyses on the NMC grid are used as guess fields for the ATOLL and 200-mb analyses. These NMC analyses are currently determined by the Flattery and Hough spectral analysis technique (Cooley, 1974). Incorporated in the analyses are height and wind data from raobs, aircraft and satellite winds, and height data derived from SIRS (Satellite Infra-Red Spectrometer) satellite temperature soundings. Corrections to the guess fields are made utilizing only aircraft data and satellite and rawinsonde winds available at NHC when the model is run.

Once the grid point values have been determined, the u (eastward) and v (northward) components of the wind at the SANBAR bogus points are obtained by interpolation from these values. The mean tropospheric wind components are then calculated from regression equations. Pike (1975) developed regression equations for computing the mean zonal and meridional components using winds at 850 mb and 200 mb as predictors. (The ATOLL level winds derived from the scanning process are used in actual applications to represent the 850-mb level winds.) Pike's derivation involved a small data sample from the Gulf of Mexico, the Caribbean Sea, and the western Atlantic Ocean. Adams and Sanders (1975) developed comparable regression equations using a larger data sample than used by Pike and including data not only from the above three geographical areas but also from the Pacific. Pike's regression

equations and those developed by Adams and Sanders are shown in Table 1. Since Pike's equations were used operationally at NHC in 1975, his equations were also used in the reruns discussed in this report. Adams's and Sanders's regression equations are now being used operationally at NHC.

After the components of the mean tropospheric wind are determined at the bogus points and at each reporting station, the mean winds at the SANBAR grid points are obtained following a statistical procedure developed by Eddy (1967). This technique provides a set of multiple regression equations with each grid point value as the predictand and the nearby bogus and rawinsonde winds as predictors. The procedure is discussed in Appendix B.

The SANBAR numerical grid extends from 36.5°W to 123.5°W longitude and from the equator to 55°N latitude on a Mercator projection true at 22.5°N. It consists of a 45 x 59 array of 2655 grid points, with a 154-kilometer mesh length at 22.5°N. The mean grid point winds which result from the Eddy analysis are used as input to the SANBAR hurricane track forecast program to obtain initial stream-function and vorticity fields over the SANBAR grid.

WIND ANALYSIS WITHIN THE INFLUENCE DISTANCE OF THE STORM

Wind analysis near the storm center is difficult not only because data are usually scarce in this area, but also

TABLE 1. Regression equations for zonal and meridional components (knots) of mean tropospheric wind, based on rawinsonde observations at 850 mb and 200 mb.

Pike (June - November)

$$\hat{u}_{1000-100} = -0.512 + 0.561u_{850} + 0.399u_{200}$$

$$\hat{v}_{1000-100} = 0.574 + 0.269v_{850} + 0.265v_{200}$$

Adams and Sanders (June - October)

$$\hat{u}_{1000-100} = 0.394 + 0.530u_{850} + 0.374u_{250}$$

$$\hat{v}_{1000-100} = -0.513 + 0.450v_{850} + 0.327v_{250}$$

Adams and Sanders (June - August)

$$\hat{u}_{1000-100} = 0.268 + 0.538u_{850} + 0.355u_{250}$$

$$\hat{v}_{1000-100} = -0.515 + 0.437v_{850} + 0.322v_{250}$$

Adams and Sanders (September - October)

$$\hat{u}_{1000-100} = 0.581 + 0.521u_{850} + 0.386u_{250}$$

$$\hat{v}_{1000-100} = -0.451 + 0.467v_{850} + 0.332v_{250}$$

because any observed winds near the storm are affected by the storm circulation and therefore do not represent the large-scale tropospheric flow required for the model. A realistic initial flow pattern must be produced in this region, and yet the storm itself must also be represented in a reasonable way.

Winds within the influence distance of the storm, usually taken as 300 n mi, are currently obtained by a procedure developed by Pike (1972a). Winds in this region are regarded as the vector sum of an idealized axisymmetric vortex and a steering flow, which is equal to the observed initial storm motion. The vortex vector is obtained on the basis of the size and intensity of the storm.¹ The location of the storm center is determined from the surface analysis and any available reconnaissance aircraft information.

Any rawinsonde or bogus point wind within the influence distance is discarded and replaced by the steering flow value. This wind is then used in the Eddy statistical analysis to determine the wind at relevant grid points outside the area

¹The vortex vector, v_e , is equal to the symmetric tangential wind determined from the following formula:

$$v_e = 0.72 V_{\max} \left[\sin \left\{ \pi \left(\frac{r}{r_m} \right)^{\left(\ln 0.5 / \ln (r_e / r_m) \right)} \right\} \right]^{1.5}$$

where V_{\max} = maximum observed storm wind speed

r = distance from the storm center

r_m = maximum influence distance

r_e = distance from the storm center to the maximum wind (usually taken as 20 n mi)

influenced by the storm. At all grid points within the influence distance, an appropriate wind is forced in according to Pike's formulation.

A REVISED ANALYSIS TECHNIQUE FOR USE IN OCEANIC REGIONS

Although the NHC grid with a mesh length of 90 n mi was originally used in the scanning procedure to obtain ATOLL and 200-mb analyses from the first guess fields, these analyses are now performed at NHC directly on the SANBAR computational grid. In light of this circumstance, use of the 44 bogus points in the analysis procedure seemed pointless.¹ It would seem that more and better use could be made of the data which is available in oceanic regions if the regression equations were applied directly to the analyzed data at the SANBAR computational grid.

Cases were therefore selected from the operational SANBAR forecasts to be rerun using this new analysis procedure. In these revised forecasts, the elliptical scanning technique was carried out on the SANBAR grid to obtain zonal and meridional wind components at the ATOLL and 200-mb levels at the SANBAR grid points. The mean u and v components were then obtained at each grid point using Pike's regression equations. Two steps in the original analysis procedure were thereby eliminated - the interpolation from the grid to obtain bogus

¹Except north of 45°N latitude which is the northern limit of the ATOLL and 200-mb analyses.

point winds and the Eddy analysis using these bogus winds to obtain u and v components at the grid points.

The revised technique eliminates the loss of information which occurs in obtaining the bogus winds from the grid point winds. Also, the satellite data and the aircraft and ship observations which are available in oceanic regions enter the analysis program more directly than in the original procedure. Although there is no way of knowing the reliability or accuracy of the height data used in the NMC analyses used as first guess fields, this data, which now also enters the model more directly, can be very useful in determining the large-scale flow at high latitudes as shown by Sanders and Gordon (1976). In tropical areas, height data is not reliable. At low latitudes, heights are nearly constant, although data would indicate variability in heights due to observational errors.

In the rerun forecasts, the Eddy statistical technique continued to be performed over land areas and oceanic regions adjacent to the coastline. In these areas rawinsonde observations are plentiful, and the investigations of King (1966) and Ahn (1967) showed that the 10 mandatory levels represent an optimum vertical sample from which to work.

The location of the boundary between the region in which the Eddy analysis would continue to be performed and the region in which the new analysis technique would be carried out was determined using a map presented by Sanders et al.(1975)

as a guide. This map (Figure 2) indicates the unexplained variances in the analysis of the zonal wind component from its mean. This map could not be used exactly as presented here for determination of the boundary location for two reasons. First, in determining the unexplained variances, the bogus points were considered to be actual rawinsonde observations. Second, many of the stations used no longer exist, and new stations have been added since this map was constructed. However, a modified version of this map, based on a recent station list and making no reference to bogus points, was used to determine the location of the boundary.

The unexplained variance at a particular grid point depends upon the distance between raob stations as well as the distance from each raob to the grid point. The unexplained variance at grid points near actual raobs is smaller if the nearby raobs, rather than the winds determined from the ATOLL and 200-mb analyses, are used to determine the grid point winds. The use of only 2 levels in the new analysis method, rather than 10 levels as used at raob stations, will in itself increase the unexplained variance. The unexplained variances are discussed in more detail in a report by Adams and Sanders (1975).

Comparisons were made of the estimated unexplained variances at the grid points using the two different analysis methods. In the final analysis, the boundary of the Eddy

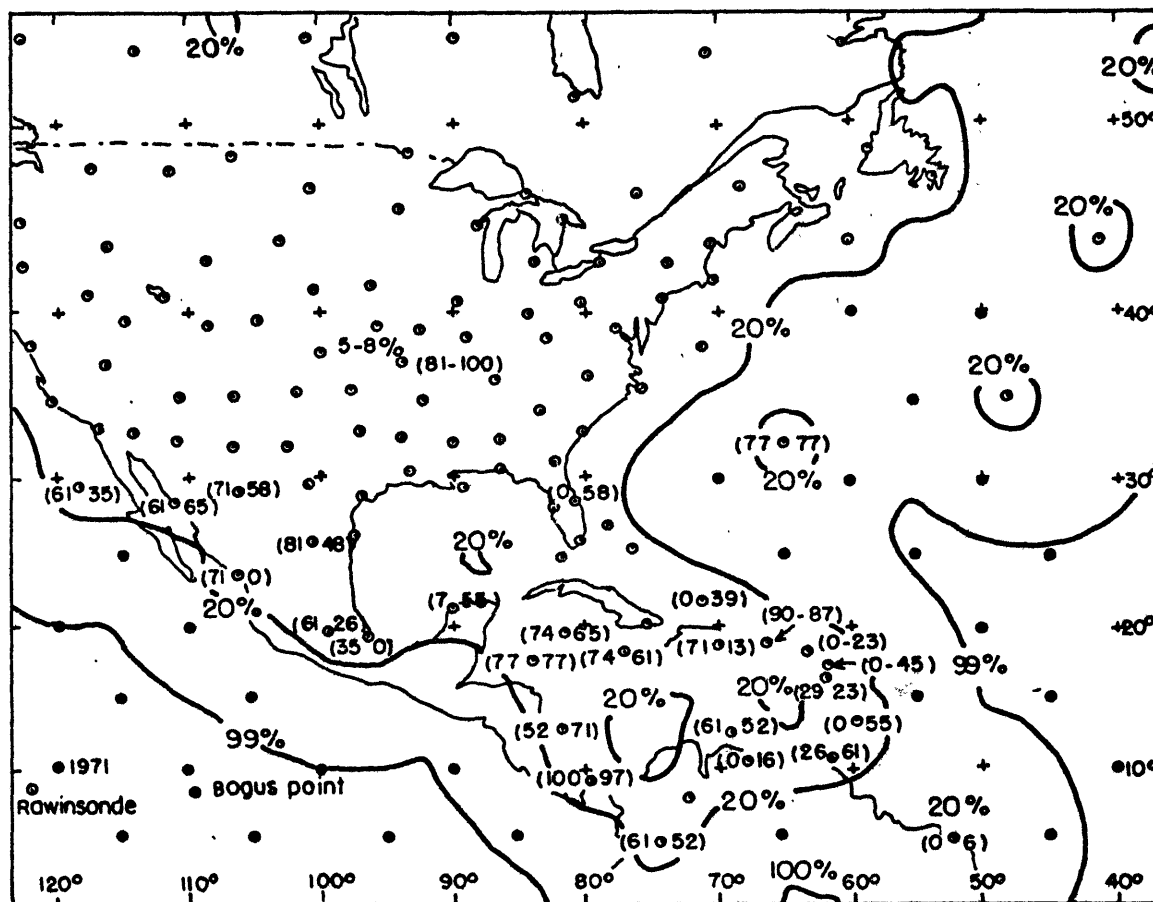


Figure 2. Map of unexplained variance in the analysis of the deviation of the zonal wind component from its zonal mean, given rawinsonde observations at the locations shown by the circled dots. Numbers in parentheses are percentages of possible observations in a recent month available in useful form at NMC for 0000GMT to the left and 1200GMT to the right of the station. (From Sanders *et al.*, 1975).

statistical analysis was taken approximately along the 15 to 20 percent unexplained variance line. In areas of lower unexplained variance, the Eddy analysis continued to be used; in areas of higher unexplained variance, the new analysis method was carried out. Figure 3 shows this boundary. Also shown in this figure are those stations which were added in the determination of the boundary and the former stations which were ignored. (Although a new set of stations was used in determining the boundary location, it was not possible to make the corrections to the station list at NHC before the selected cases were rerun using the revised analysis procedure.)

OPERATIONAL SANBAR FORECASTS OF 1975

During the 1975 hurricane season, eight tropical cyclones were named by NHC. The paths of these storms are shown in Figure 4. These represent the "best-tracks" which are determined after careful post-analysis and represent a compromise between given observational positions and the desire to obtain a relatively smooth path by elimination of small-scale perturbations of the storm center. Seventy-eight SANBAR forecasts were made operationally at NHC in 1975. Mean position errors for each of the named storms and for a total of 74 of the 78 cases are shown in Table 2.¹ As the forecast

¹Four of the 78 cases were excluded in the statistics for several reasons unrelated to the accuracy of the forecasts.

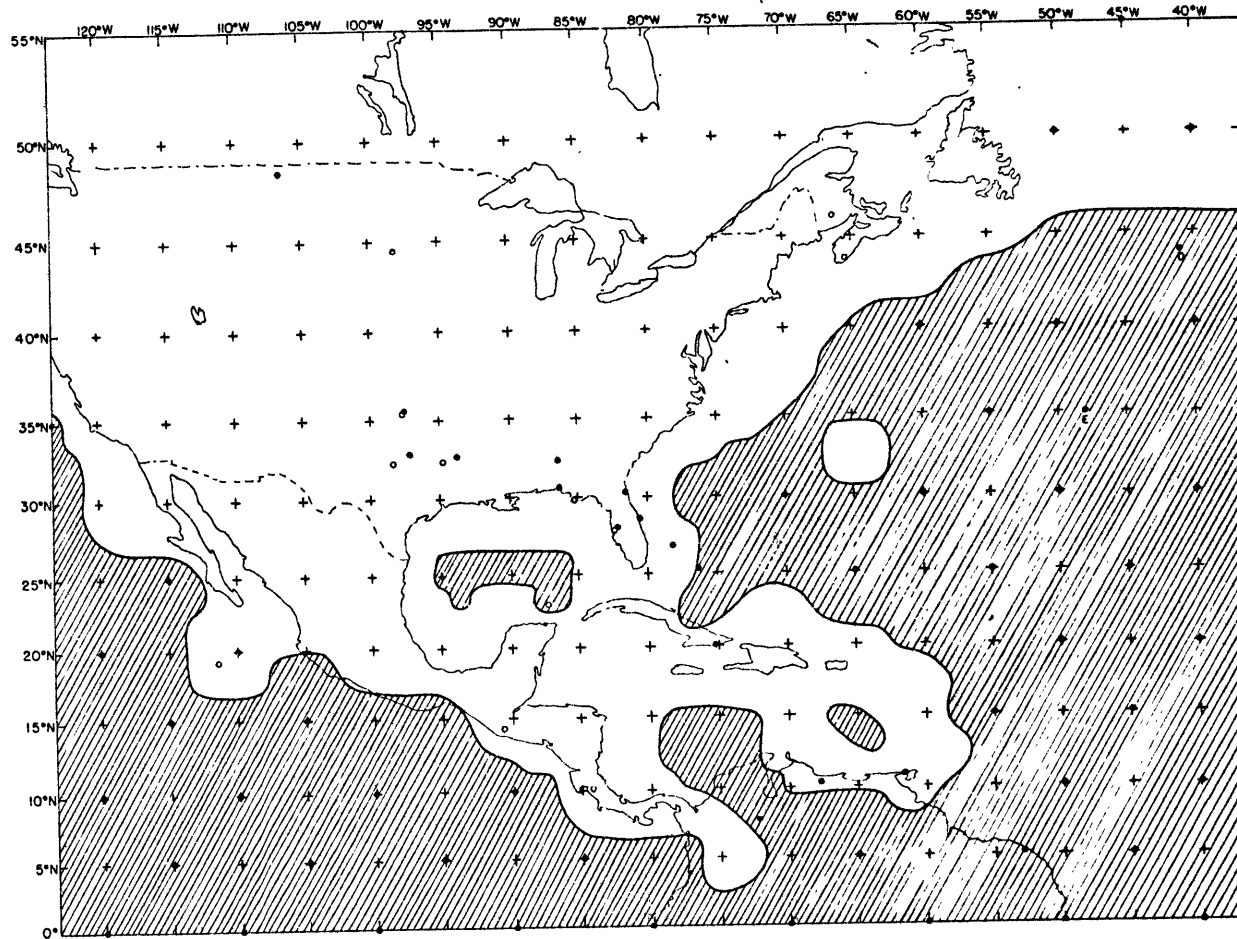


Figure 3. Map showing areas in which the Eddy analysis continued to be performed and regions in which the new analysis procedure was carried out (hatched areas) in the rerun forecasts. Open circles indicate locations of rawinsonde stations which have been added to the NHC station list since Figure 2 was constructed. Closed circles indicate former stations and bogus points not considered in determining the boundary location.

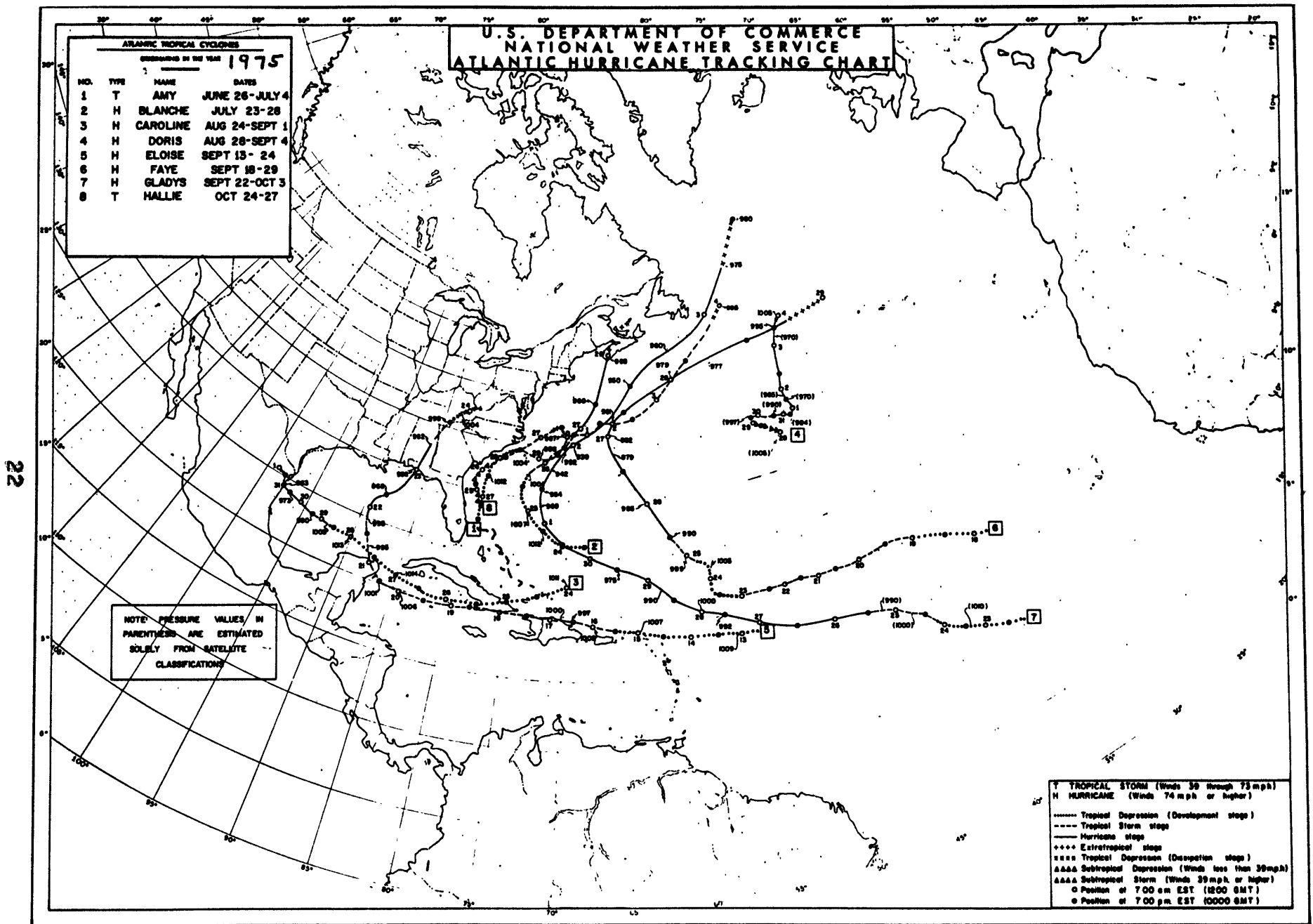


Figure 4. Best tracks of 1975 storms.

TABLE 2. Mean position errors (nautical miles) for operational SANBAR forecasts.

	<u>00 hr</u>	<u>12 hr</u>	<u>24 hr</u>	<u>36 hr</u>	<u>48 hr</u>	<u>72 hr</u>
Amy	8 (7)	72 (6)	107 (5)	117 (5)	197 (5)	338 (3)
Blanche	16 (4)	53 (3)	101 (2)	135 (1)	—	—
Caroline	7 (5)	33 (4)	73 (3)	116 (2)	152 (1)	—
Doris	11 (10)	72 (9)	104 (8)	174 (7)	240 (6)	369 (4)
Eloise	18 (15)	60 (14)	95 (13)	134 (12)	198 (11)	283 (9)
Faye	19 (14)	73 (13)	151 (11)	218 (9)	268 (7)	483 (5)
Gladys	11 (17)	76 (17)	144 (16)	233 (15)	347 (14)	459 (12)
Hallie	46 (2)	65 (1)	—	—	—	—
<u>Mean</u>	15 (74)	67 (67)	121 (58)	181 (51)	261 (44)	393 (33)

()Number in sample

range increases, the number of verifications, taken from best-track positions, decreases due to the passage of the storm inland or its movement out to sea where it no longer threatens the North American coastline. Tracks ceased in a few cases due to a significant weakening of the storm. The position errors also show substantial growth as the forecast range increases. Large errors at early times are usually due to inaccurate positioning of the storm center at the initial time and to an incorrect estimate of the initial storm direction and velocity. Large errors at later forecast ranges usually reflect the inaccuracy in prediction of the large-scale flow pattern.

None of the mean errors for individual storms at any forecast range differed significantly from the total means for the entire sample at the same range.¹ This would seem to indicate that none of the storms was easier or more difficult to predict than any other storm. As can be seen from Figure 4, none of the storm tracks of this year were eccentric, involving cusps, loops, or sudden starts and stops. If more irregular tracks had occurred, significant differences in the means would have appeared, indicating a variation in prediction difficulty.

It is interesting to note the existence of errors in the initial positioning of the storm center. This is the

¹Actually, one significant difference occurred. The mean for Hallie at 00 hr differed significantly from the total mean at that time (at the 10% level).

result of best-track positions being determined after the fact whereas forecast positions must be determined using only the information gathered prior to the initial time. The largest error, 46 n mi, occurred for a Hallie forecast with substantial errors also occurring for Blanche, Eloise, and Faye. The effects of the initial displacement would be maximum near the initial time and probably vanish by 48 hours.

Speed and direction errors were also calculated for each forecast for the first and second 24-hour periods. The speed error was taken as the difference between the best-track speed and the SANBAR forecast speed during the 24-hour period; the direction error was defined as the perpendicular distance from the forecast position to the observed displacement vector. Figure 5 illustrates the definitions of these errors. Mean magnitudes and algebraic means were computed for both speed and direction errors; The results are shown in Tables 3 and 4, respectively. As expected, for most of the storm means and for the total sample means, the speed and direction errors were much greater for the second 24-hour period than for the first.

Table 4 reveals some interesting biases. A negative speed error indicates a slow bias in the forecast; a negative direction error indicates a left bias. Overall, the forecasts show a slow bias and displacement to the left of the observed track. Also, all individual storms showed a slow bias during the first and second 24-hour periods, except

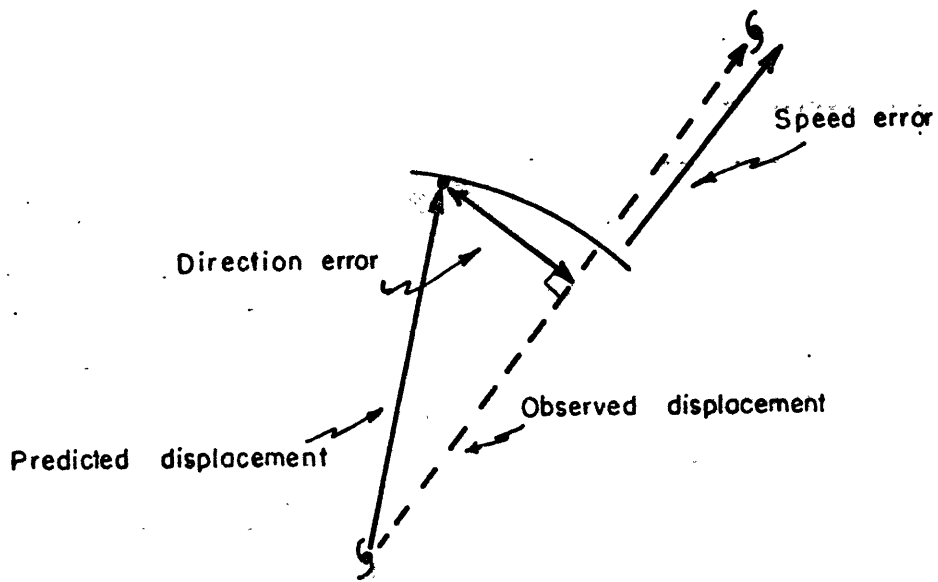


Figure 5. Sketch illustrating direction and speed errors.

TABLE 3. Mean magnitudes of speed and direction errors for operational SANBAR forecasts in 1975.

	SPEED ERRORS(n mi)		DIRECTION ERRORS(n mi)	
	<u>00-24hr</u>	<u>24-48hr</u>	<u>00-24hr</u>	<u>24-48hr</u>
Amy	34 (5)	96 (5)	93 (5)	74 (5)
Blanche	48 (2)	—	54 (2)	—
Caroline	55 (3)	72 (1)	18 (3)	74 (1)
Doris	60 (8)	60 (6)	47 (8)	75 (6)
Eloise	46 (13)	41 (11)	70 (13)	101 (11)
Faye	120 (11)	137 (7)	67 (11)	80 (7)
Gladys	98 (16)	166 (14)	82 (16)	107 (14)
Hallie	—	—	—	—
<u>Mean</u>	77 (58)	106 (44)	68 (58)	92 (44)

()Number in sample

TABLE 4. Algebraic means of speed and direction errors for operational SANBAR forecasts in 1975.

	SPEED ERRORS(n mi)		DIRECTION ERRORS(n mi)	
	<u>00-24hr</u>	<u>24-48hr</u>	<u>00-24hr</u>	<u>24-48hr</u>
Amy	-5 (5)	-58 (5)	34 (5)	74 (5)
Blanche	-2 (2)	—	54 (2)	—
Caroline	-7 (3)	72 (1)	-18 (3)	-74 (1)
Doris	-31 (8)	-43 (6)	2 (8)	45 (6)
Eloise	-5 (13)	-19 (11)	-1 (13)	-72 (11)
Faye	-41 (11)	-14 (7)	-38 (11)	-38 (7)
Gladys	-79 (16)	-134 (14)	-32 (16)	-24 (14)
Hallie	—	—	—	—
<u>Mean</u>	-36 (58)	-60 (44)	-12 (58)	-19 (44)

()Number in sample

for Caroline which showed a fast bias during the second period. Left biases occurred for 4 of 7 storms during the first 24-hour period and for 4 of 6 storms during the later period.

During the period when forecasts were made, the 1975 storms tended strongly to recurve and accelerate, as can be seen in Figure 4. This was especially true for Eloise, Faye, and Gladys for which the majority of forecasts were made. (The initial storm position was north of 30°N in 31 of the 74 SANBAR forecasts.) Evidently, the model was not able to forecast accurately the large-scale flow necessary to produce these characteristics in the forecast tracks. Slow biases and left biases would probably been reduced if more of the actual tracks had been irregular.

SELECTION OF CASES TO BE RERUN

Forecasts which were to be examined and rerun using the revised analysis technique were selected from the 78 operational SANBAR forecasts made for storms in the Atlantic Ocean in 1975. Any forecasts which were made while storms were located in the extreme northern or eastern portions of the SANBAR grid were not considered, since very few data are available in these areas. Eloise, Faye, and Gladys were in the best locations for analysis. From the forecasts made for these storms, four cases with relatively small position errors and four cases with large position errors at each of three forecast ranges, 24, 48, and 72 hours, were chosen for

rerun. Additional cases were then selected from the forecasts made for Amy, Caroline, and Doris in order to include forecasts from a variety of storms having different characteristics.¹ From these three storms, 6 good and 6 bad forecasts were selected, with 2 good and 2 bad cases at each of the three forecast ranges.²

The 18 bad and 17 good selected cases are listed in Table 5 along with the storm parameters. It was expected that the bad cases would show improvement and that the good cases would be adversely affected. This would most likely occur even if the revised procedure had no real merit. However, if the improvement exceeded the deterioration, the new analysis technique would be considered helpful.

COMPARISON OF ERRORS
FOR SELECTED OPERATIONAL AND RERUN FORECASTS

Position Errors

Position errors were calculated for both the selected operational SANBAR forecasts and the rerun forecasts in which the new analysis technique was utilized. Mean position errors are shown in Tables 6 and 7. The 00-hour errors were the same for both sets of forecasts since the initial position of the

¹No Blanche or Hallie forecasts were selected. Since very few best-track positions were known, only a small number of position errors could be calculated.

²One of the good cases was not rerun because of a miscalculation in the forecast position.

TABLE 5. List of cases for revised forecasts.

STORM PARAMETERS*						
Storm	Date mo/day	Initial Time (GMT)	Max. Wind (kts)	Eye Diam. (n mi)	Oper. Dir/Spd (°/kts)	Remarks
Amy	06/30	1200	60	20	030/06	good at 48 & 72 hrs.
	07/01	0000	60	20	090/03	bad at 72 hrs.
	07/02	1200	60	20	080/05	bad at 24 hrs.
	07/03	0000	45	30	065/10	bad at 24 hrs.
Caroline	08/29	1200	55	20	284/08	good at 48 hrs.
	08/30	1200	70	10	280/07	good at 24 hrs.
Doris	08/30	1200	50	20	090/03	good at 72 hrs.
	08/31	1200	65	20	115/08	bad at 48 & 72 hrs.
	09/01	1200	75	20	075/01	bad at 48 hrs.
Eloise	09/16	0000	35	35	285/07	good at 24 & 48 hrs.
	09/16	1200	35	25	275/11	good at 48 & 72 hrs.
	09/18	0000	65	25	275/10	good at 48 & 72 hrs.
Faye	09/22	0000	45	30	275/05	good at 24 hrs.
	09/25	1200	40	30	310/09	bad at 48 & 72 hrs.
	09/26	0000	60	30	315/11	bad at 24 & 72 hrs.
	09/26	1200	65	30	325/18	good at 24 hrs.
Gladys	09/26	1200	65	30	280/12	good at 72 hrs.
	09/28	1200	75	30	270/10	bad at 24 hrs.
	09/29	0000	65	30	300/10	good at 72 hrs.
	09/30	0000	90	20	295/14	good at 48 hrs; bad at 72 hrs.
	09/30	1200	90	15	290/13	good at 24 hrs; bad at 48 & 72 hrs.
	10/01	0000	90	20	270/13	bad at 24 & 48 hrs.
	10/01	1200	90	15	340/12	bad at 48 hrs.
10/02	0000	120	12	334/20	bad at 24 hrs.	

* Radius of influence assumed 300 n mi in all cases except Gladys, 09/28, 1200GMT, and Gladys, 09/29, 0000GMT, for which radius assumed 200 n mi.

TABLE 6. Mean position errors (nautical miles) for selected operational forecasts.

	<u>00 hr</u>	<u>12 hr</u>	<u>24 hr</u>	<u>36 hr</u>	<u>48 hr</u>	<u>72 hr</u>
Amy	12 (4)	58 (4)	151 (4)	224 (3)	148 (2)	380 (2)
Caroline	6 (2)	14 (2)	40 (2)	70 (1)	152 (1)	—
Doris	7 (3)	65 (3)	123 (3)	197 (3)	277 (3)	364 (2)
Eloise	17 (3)	27 (3)	51 (3)	59 (3)	84 (3)	133 (3)
Faye	18 (4)	53 (4)	99 (4)	207 (3)	276 (3)	816 (2)
Gladys	10 (8)	63 (8)	134 (8)	281 (8)	432 (7)	547 (5)
<u>Mean</u>	12 (24)	52 (24)	111 (24)	209 (21)	283 (19)	447 (14)

()Number in sample

TABLE 7. Mean position errors (nautical miles) for rerun forecasts.

	<u>00 hr</u>	<u>12 hr</u>	<u>24 hr</u>	<u>36 hr</u>	<u>48 hr</u>	<u>72 hr</u>	<u>Total*</u>
Amy	12 (4) [0]	62 (4) [0]	159 (4) [2]	238 (3) [1]	205 (2) [0]	479 (2) [0]	(15) [3]
Caroline	6 (2)	14 (2) [2]	37 (2) [1]	47 (1) [1]	100 (1) [1]	—	(6) [5]
Doris	7 (3)	63 (3) [3]	125 (3) [1]	199 (3) [2]	289 (3) [2]	311 (2) [2]	(14) [10]
Eloise	17 (3)	31 (3) [1]	48 (3) [2]	63 (3) [1]	98 (3) [2]	164 (3) [0]	(15) [6]
Faye	18 (4)	49 (4) [3]	105 (4) [2]	208 (3) [2]	330 (3) [0]	923 (2) [0]	(16) [7]
Gladys	10 (8)	68 (8) [3]	145 (8) [1]	286 (8) [4]	440 (7) [3]	572 (5) [2]	(36) [13]
<u>Mean</u>	12 (24)	54 (24) [12]	117 (24) [9]	212 (21) [11]	302 (19) [8]	484 (14) [4]	(102) [44]

Change from the operational forecasts

+0 +2 +6 +3 +19 +37

*Total excluding 00 hr.

() Number in sample

[] Number in sample which had position errors equal to or less than those of operational forecasts.

storm center was taken to be the same in both runs. The mean position errors for the entire sample of 24 forecasts were greater at all forecast ranges for the rerun forecasts. The difference between the total means of the two forecast samples increases with time, except between 24 and 36 hours. The means for the revised forecasts, however, were not significantly different from those for the operational runs. This was true not only for the total sample means, but also for all individual storm means at all times. These results would seem to indicate that the revised analysis procedure is no better, and no worse, than the original procedure.

The number of cases in the rerun sample which had position errors equal to or less than those of the operational runs is also indicated in Table 7. Although the total sample means were greater at all ranges for the reruns, not all individual forecasts were made worse. Although the deterioration was slightly greater, overall, than the improvement, the number of forecasts which were improved by the new method was approximately equal to the number which showed deterioration at all forecast ranges except 72 hours. At this range, the new procedure caused the deterioration of 10 of the 14 forecasts. Evidently, the new technique was helpful in a large number of forecasts.

The revised technique improved a significant number of forecast positions for Caroline and Doris. For Caroline, 5 out of 6 forecast positions were improved using the new

method; for Doris, 10 out of 14 were improved. Although both of these storms occurred during late August and early September, the origin, development, and location of these storms were quite different. Caroline developed from a tropical depression off the west coast of Africa and reached hurricane intensity upon reaching the Gulf of Mexico on the 30th of August. The storm then intensified rapidly and made landfall near Brownsville, Texas on the 31st. It weakened rapidly after landfall and dissipated in northeastern Mexico. Doris, on the other hand, developed in the mid-Atlantic and was designated a subtropical storm before being named. The storm, which reached hurricane strength on August 30th, moved slowly west, then east, and finally north, never becoming a threat to any land areas (Hebert, 1975).

During the period in which the two Caroline forecasts were made, the storm was moving entirely within the region of Eddy analysis. The initial positions were just west of the area in the Gulf of Mexico where the new analysis technique was carried out (see Figure 3). Evidently, the initial analysis was improved using the new method, particularly in the Gulf.

The Doris forecasts were made while the storm was far out to sea, totally within the region in which the new procedure was carried out. The fact that these forecasts were improved indicates again that the new analysis method is able to generate a better initial large-scale flow pattern than

the operational procedure in some instances.

The storm which showed the greatest percentage of deterioration in forecast positions using the new analysis method was Amy. Of 15 position errors, only 3 were improved by the new procedure. Other problems appeared to occur for the revised technique during the later forecast ranges for Eloise and Faye and at most ranges for Gladys.

The deterioration observed in the Eloise forecasts was expected since excellent operational forecasts were made for all three selected cases. Although slight deterioration did occur, the fact that the revised procedure was also able to produce excellent forecasts is encouraging.

Many of the selected forecasts made for Amy, Faye, and Gladys were made while the storms were moving along the boundary which separates the two different analysis procedures. It appears, at first glance, that discontinuities which occur along this boundary may have been partially responsible for the deterioration of the revised forecasts made for these storms. This, however, was probably not the case. An investigation of the rerun forecasts revealed a number of good forecasts in instances where the storm moved along or across the boundary. Amy, Faye, and Gladys were also storms which recurved in the Atlantic and accelerated northeastward (see Figure 4). It is difficult to know precisely how much of the deterioration was due to their location near the boundary and to the characteristics of their movement. Several

forecasts made for these storms are examined in detail later on in this report.

As previously mentioned, it was expected that the bad cases would show improvement and that the good cases would be adversely effected. Overall, however, the good cases remained approximately the same, neither improving nor deteriorating, when the revised procedure was used. The greatest number of deteriorated good cases occurred at the 24-hour range. Overall, the bad cases worsened, with the primary problem occurring at the 72-hour range. The reason for these unexpected results is not immediately apparent.

Speed Errors

Mean magnitudes and algebraic means of speed errors are summarized in Tables 8 and 9. The speed errors are given in nautical miles per 24 hours and were calculated for three consecutive 24-hour periods. As can be seen from these tables, the means for the total sample for both the original runs and the reruns increase with increasing forecast range. Although the mean speed error for the rerun sample was greater than that for the operational sample for each time period, none of the rerun means were significantly different from the operational means. This was true not only for the entire sample but also for individual storm means.

Both the operational runs and the rerun forecasts showed a slow bias for all three 24-hour periods. For the operational

TABLE 8. Mean magnitudes of speed errors
(nautical miles per 24 hours) for selected
operational forecasts and rerun forecasts.

	OPERATIONAL			RERUN		
	<u>00-24hr</u>	<u>24-48hr</u>	<u>48-72hr</u>	<u>00-24hr</u>	<u>24-48hr</u>	<u>48-72hr</u>
Amy	126 (4)	72 (2)	180 (2)	138 (4)	48 (2)	168 (2)
Caroline	36 (2)	72 (1)	—	24 (2)	12 (1)	—
Doris	96 (3)	72 (3)	144 (2)	88 (3)	64 (3)	120 (2)
Eloise	24 (3)	40 (3)	48 (3)	8 (3)	32 (3)	40 (3)
Faye	90 (4)	112 (3)	444 (2)	90 (4)	176 (3)	528 (2)
Gladys	111 (8)	226 (7)	326 (5)	135 (8)	237 (7)	370 (5)
<u>Mean</u>	91 (24)	130 (19)	237 (14)	97 (24)	136 (19)	257 (14)

()Number in sample

TABLE 9. Algebraic means of speed errors
(nautical miles per 24 hours) for selected
operational forecasts and rerun forecasts.

	OPERATIONAL			RERUN		
	<u>00-24hr</u>	<u>24-48hr</u>	<u>48-72hr</u>	<u>00-24hr</u>	<u>24-48hr</u>	<u>48-72hr</u>
Amy	-114 (4)	-24 (2)	-180 (2)	-114 (4)	0 (2)	-168 (2)
Caroline	36 (2)	72 (1)	—	24 (2)	12 (1)	—
Doris	-32 (3)	-56 (3)	-144 (2)	-24 (3)	-64 (3)	-120 (2)
Eloise	8 (3)	-40 (3)	-48 (3)	-8 (3)	-32 (3)	-40 (3)
Faye	-90 (4)	-112 (3)	-444 (2)	-90 (4)	-176 (3)	-528 (2)
Gladys	-111 (8)	-226 (7)	-326 (5)	-135 (8)	-237 (7)	-370 (5)
<u>Mean</u>	-71 (24)	-115 (19)	-237 (14)	-81 (24)	-129 (19)	-257 (14)

()Number in sample

runs, all individual storms showed a slow bias, except Caroline during the 00-24 hour and 24-48 hour periods and Eloise during the 00-24 hour range. In the rerun forecasts, Amy during the 24-48 hour period and Caroline during the 00-24 hour and 24-48 hour periods were the only individual means showing a fast bias. Thus, both sets of forecasts were basically slow for 5 of the 6 storms sampled. As mentioned earlier, many of the 1975 storms tended strongly to recurve and accelerate when the SANBAR forecasts were made. The operational forecasts were unable to accelerate the storms to a sufficient degree. This was also the case for the revised forecasts.

It is interesting to note that the mean magnitudes of the speed errors for individual storms were less for the reruns, except for the first 24-hour period of Amy, the second and third periods of Faye, and for all time periods of Gladys. The algebraic means for individual storms were also less for the reruns, except for Doris during the second period, Faye during the second and third periods, and Gladys during all time periods. It appears, therefore, that the increase in speed errors seen in the reruns was primarily due to forecasts for Faye and Gladys, just two of the six storms sampled. The tracks of these storms were very similar, showing westward movement across the Atlantic Ocean, recurvature off the coast of the United States, and then acceleration to the northeast. Evidently, the revised pro-

cedure was even less successful than the original one in accelerating the storms during and after recurvature.

There appears to be an extra element of slowness in the reruns when considering the total samples. Of the 24 cases for which 00-24 hour speeds were calculated, the reruns were slower than the original runs in 11 cases. For the 24-48 hour period, 10 of the 19 cases showed lower speeds. During the final period, 48-72 hours, out of 14 cases, 8 reruns were slower. The percentage of slower rerun cases increased with time, and in only 8 out of a total of 57 cases were the rerun speeds greater than the operational ones. The reasons for this increased slowness are not clear.

Direction Errors

Direction errors were calculated for both the selected operational forecasts and the revised forecasts. Mean magnitudes of the direction errors are summarized in Table 10. For the total sample, directions were improved in the reruns for the first and last 24-hour periods, although they deteriorated during the 24-48 hour interval. The individual storm means varied widely, being better than the original runs in some cases and worse in others. Neither the total means nor the individual storm means for the rerun forecasts were significantly different from those of the operational forecasts, except for the 48-72 hour means for Faye which were significantly different at the 10 percent level. Notice in this

TABLE 10. Mean magnitudes of direction errors (n mi) for selected operational forecasts and rerun forecasts.

	OPERATIONAL			RERUN		
	<u>00-24hr</u>	<u>24-48hr</u>	<u>48-72hr</u>	<u>00-24hr</u>	<u>24-48hr</u>	<u>48-72hr</u>
Amy	36 (4)	62 (2)	56 (2)	28 (4)	142 (2)	116 (2)
Caroline	15 (2)	74 (1)	—	27 (2)	29 (1)	—
Doris	43 (3)	56 (3)	23 (2)	46 (3)	62 (3)	45 (2)
Eloise	27 (3)	39 (3)	56 (3)	25 (3)	62 (3)	36 (3)
Faye	19 (4)	94 (3)	207 (2)	24 (4)	112 (3)	127 (2)
Gladys	86 (8)	105 (7)	88 (5)	80 (8)	122 (7)	69 (5)
<u>Mean</u>	48 (24)	79 (19)	84 (14)	46 (24)	99 (19)	73 (14)

()Number in sample

particular instance that the reruns showed great improvement over the original runs.

Table 11 summarizes the algebraic means for the selected cases. Again, the individual storm means varied greatly and only the 48-72 hour means for Faye were significantly different. For the total sample, the rerun forecasts showed improvement over the original runs during each 24-hour period, although the means were not significantly different for the two sets of forecasts.

These results indicate an overall improvement in directions for the revised forecasts. The fact that a large number of the forecasts were made while storms were recurring suggests that the new analysis method may generate better forecasts in such instances. This is also indicated by the significant differences which occurred in the direction errors for Faye during the 48-72 hour period, since Faye displayed strong recurvature during the forecasts periods.

RESULTS OF THE EXAMINATION OF THE RERUN FORECASTS

The selected forecasts were thoroughly examined to determine any problems which might have negated the improvement expected by using the new analysis method. The results of this examination are discussed here.

Loss of the Stream-function Minimum

The loss of the stream-function minimum in one set of

TABLE 11. Algebraic means of direction errors (n mi) for selected operational forecasts and rerun forecasts.

	OPERATIONAL			RERUN		
	<u>00-24hr</u>	<u>24-48hr</u>	<u>48-72hr</u>	<u>00-24hr</u>	<u>24-48hr</u>	<u>48-72hr</u>
Amy	3 (4)	62 (2)	56 (2)	28 (4)	142 (2)	116 (2)
Caroline	-15 (2)	-74 (1)	—	-2 (2)	-29 (1)	—
Doris	23 (3)	44 (3)	23 (2)	22 (3)	47 (3)	45 (2)
Eloise	27 (3)	-11 (3)	-33 (3)	25 (3)	-8 (3)	19 (3)
Faye	-19 (4)	-94 (3)	-207 (2)	-24 (4)	-112 (3)	-127 (2)
Gladys	-72 (8)	-82 (7)	-88 (5)	-56 (8)	-29 (7)	-54 (5)
<u>Mean</u>	-22 (24)	-37 (19)	-57 (14)	-12 (24)	-9 (19)	-10 (14)

()Number in sample

forecasts and not in the other set was partially responsible for the greater mean position errors observed in the rerun forecasts. The initial storm position is determined from surface analyses and any available reconnaissance aircraft information. Subsequent forecast positions are obtained by first determining the mean of the absolute vorticity maximum and the stream-function minimum positions. This mean position is then adjusted by a vector correction equal to the vector discrepancy between the specified initial position and the mean of the absolute vorticity maximum and stream-function minimum positions at the initial time. In an examination of the 74 SANBAR forecasts of 1975, Sanders and Gordon (1976) showed that, on the average, this initial correction is toward the northeast, because the average storm is embedded in a southeasterly large-scale flow and the stream-function minimum is too far to the southwest. The average vector correction was small, ranging from 5 to 11 nautical miles.

Often during SANBAR forecasts, the stream-function minimum is lost. This may be the result of truncation error or the strengthening of the large-scale flow near the storm. The vorticity maximum is then taken to be the unadjusted mean position to which the vector correction is applied. A spurious movement to the right is apparent in the forecast track when this occurs. The loss of the stream-function

minimum will usually improve the forecast position if the forecast track shows a left bias; if the forecast track shows a right bias, a deterioration of the forecast track will result.

The effect of the stream-function minimum loss is illustrated by examination of the SANBAR forecast for Faye, September 25th, 1200GMT. Faye developed from a tropical disturbance which moved westward from the African coast. As shown in Figure 4, Faye was still classified as a tropical storm at the initial time of this forecast. Twelve hours later the storm had reached hurricane strength, and hurricane intensity was maintained during the next 72 hours. The storm began recurvature on the 24th and continued to move northwestward until the 27th, when it came under the influence of strong westerly flow in middle latitudes. It then recurved again and accelerated to the northeast.

Figure 6 shows the best-track and SANBAR forecast tracks for Faye beginning at 1200GMT on the 25th. Position errors for the operational and rerun SANBAR forecasts are shown below in Table 12. Except at 12 hours, the position errors

TABLE 12. Position errors (n mi) for SANBAR forecasts for Faye, September 25, 1200GMT.

	<u>00 hr</u>	<u>12 hr</u>	<u>24 hr</u>	<u>36 hr</u>	<u>48 hr</u>	<u>72 hr</u>
Operational	17	48	126	232	351	671
Rerun	17	44	162	306	468	819
Change from the operational	0	+4	+36	+74	+117	+148

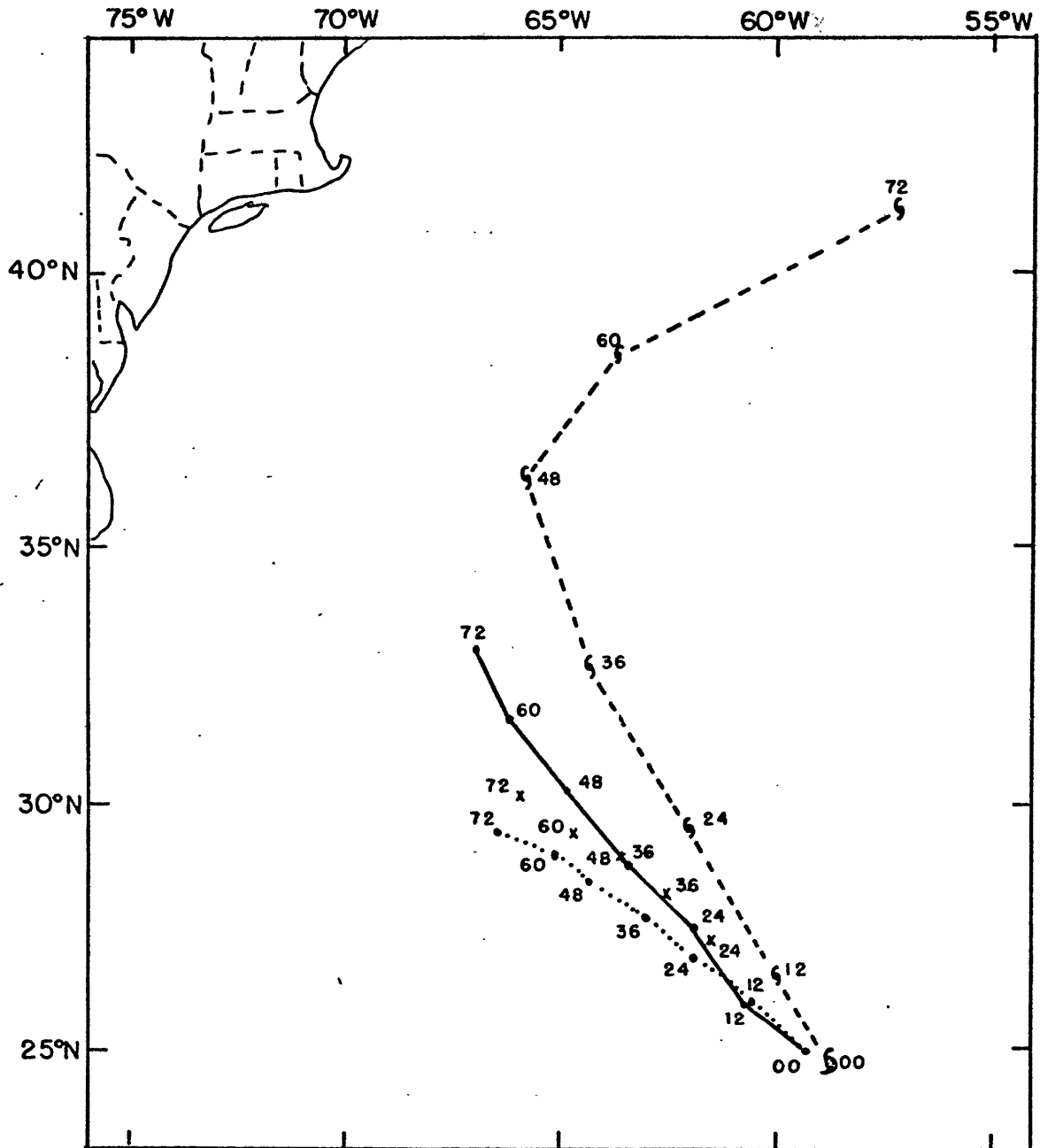


Figure 6. Tracks of Faye, September 25, 1200GMT. Dashed lines indicate observed track; solid lines, operational track; and dotted lines, revised forecast track. Dots show forecast positions, labelled with the appropriate number of hours after initial time. Corresponding observed positions are shown by hurricane symbols, with open centers indicating tropical storm strength and closed centers indicating hurricane intensity. The x's show approximate storm positions which would have been predicted if the stream-function minimum had been lost in the rerun.

were greater for the rerun forecasts than for the operational run, and the differences increased with increasing forecast range. The initial position error was very large and probably accounted for much of the position error at 12 hours. As seen in Figure 6, although both forecasts showed a slow bias, the rerun forecast was much slower than the operational one, except at the 12-hour position. After the first 12 hours, the storm began to accelerate and forecast speeds were at least 50 percent slower than observed speeds. Although the operational forecast showed a left bias, the rerun forecast, which utilized the new analysis procedure over oceanic regions, indicated storm positions even farther to the left of the observed track.

The stream-function minimum was lost after 12 hours in the operational forecast. The jog to the right resulting from this loss is apparent in the operational track shown in Figure 6. Since the forecast exhibited a left bias, this movement improved each successive forecast position. The rerun did not receive this benefit since the stream-function minimum was retained during the entire forecast. The x's in Figure 6 indicate the approximate storm positions which the rerun would have predicted if the stream-function minimum had been lost during the forecast. In that event, the rerun forecast track would have been close to the operational track at least through 36 hours. Forecast directions would have been more nearly the same, although forecast speeds would still

have been much lower for the rerun than for the operational run. Overall, the difference between position errors for the two forecasts would have been smaller.

The initial stream-function pattern for the operational and rerun SANBAR forecasts are shown in Figure 7. (The location of Gladys is also shown in this figure, although it was not one of the cases selected for rerun.) Overall, the two analyses are very similar, particularly in the vicinity of the storm. If the stream-function minimum had been lost during the rerun, the storm would probably have been forecast to move slightly faster, although no significant increase in speed would have occurred. Southeast of the storm, substantial differences appear in the stream-function patterns. Here, the pattern indicates a weaker flow in the rerun forecast. This weaker flow is substantiated by the winds displayed in Figure 8. Mean SANBAR grid point winds used in the determination of the initial stream-function field for the rerun forecast are shown in this figure. Also indicated are the mean bogus winds used in the Eddy analysis in the operational forecast to obtain grid point winds not shown here. All the winds within the influence distance of the storm, including those at bogus points 14 and 23, were discarded, and winds appropriate to the storm parameters (see Table 5) were forced in, as previously explained. All the winds within the influence distance were therefore the same for both SANBAR forecasts.

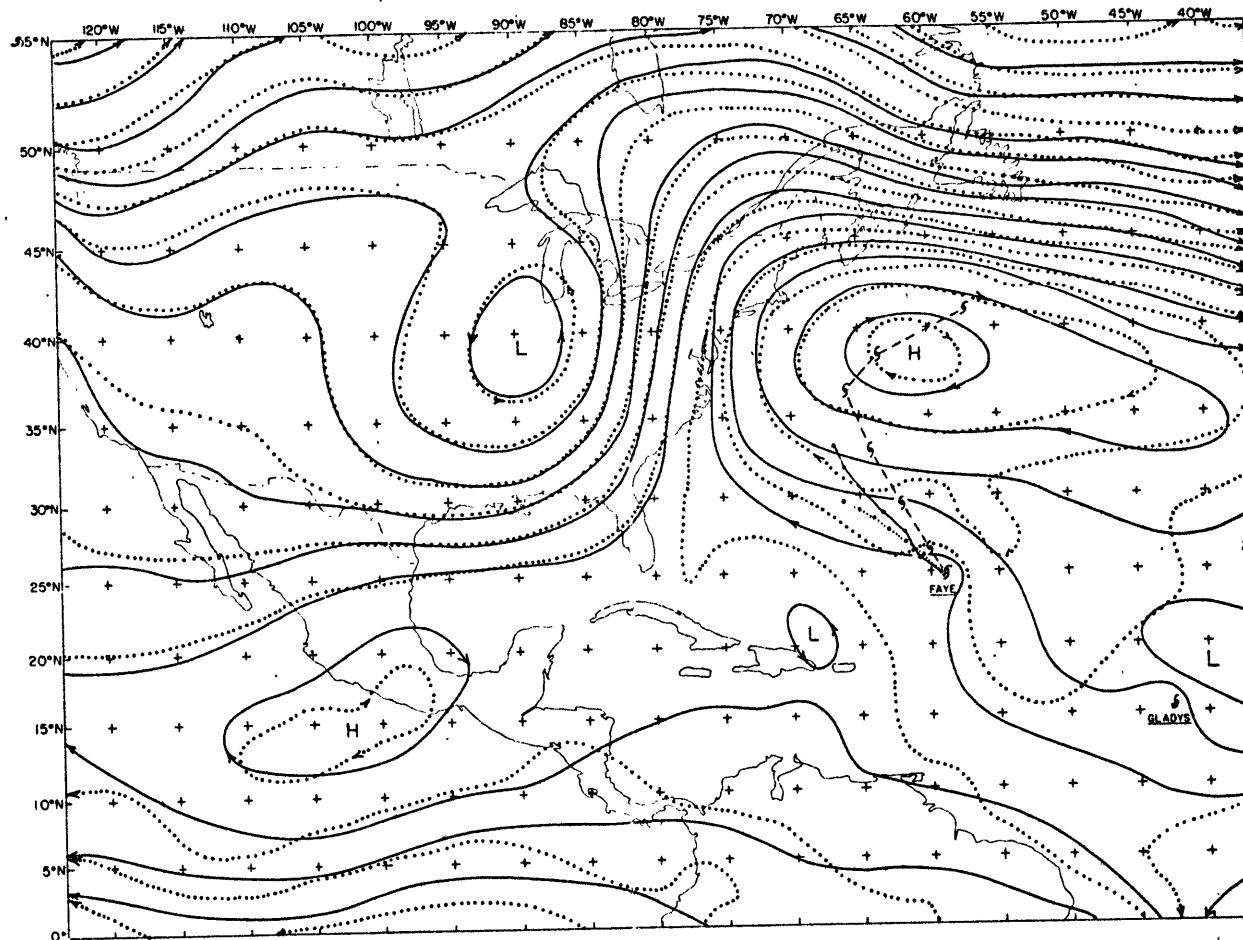


Figure 7. Initial analyses of large-scale flow pattern, September 25, 1200GMT, for the operational SANBAR run (solid lines) and for the rerun forecast (dotted lines). Lines are isopleths of stream-function at intervals of $300 \times 10^4 \text{ m}^2 \text{ s}^{-1}$. Best-track and forecast tracks are also shown, with the notation the same as Figure 6.

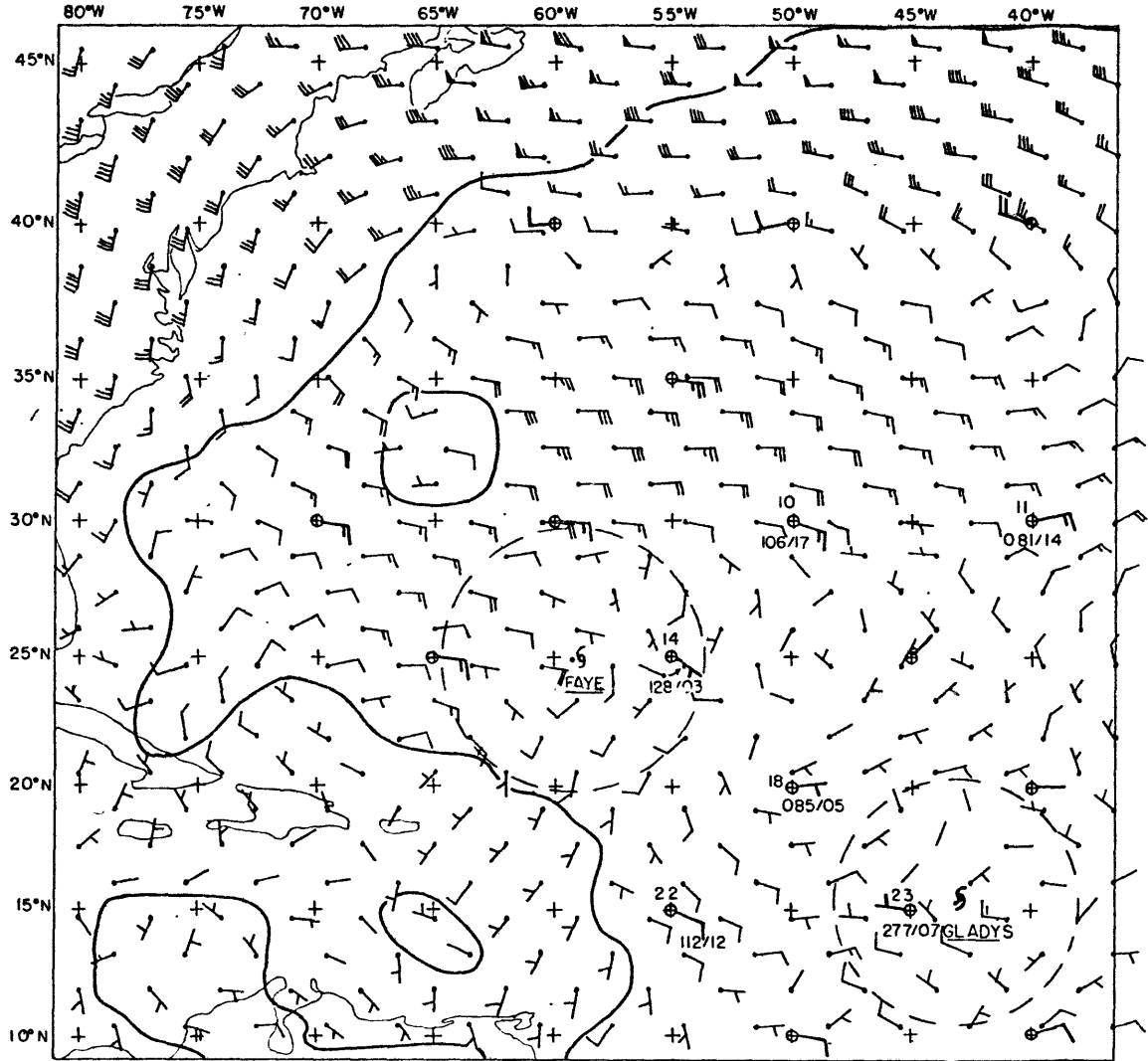


Figure 8. Bogus winds and SANBAR grid point winds for the forecasts beginning September 25, 1200GMT. Circled x's indicate bogus winds. Radius of influence is shown by the dashed circle. Solid lines separate areas of different analysis techniques.

At bogus points 10, 11, 18, and 22 the mean winds were generally stronger than the winds at the surrounding grid points. This indicates a stronger mean flow in the operational run than in the rerun. It is difficult to account for this slowness, which was also apparent in a large number of the other reruns. Since the use of bogus points results in a loss of information, it seems reasonable to assume that a more accurate initial stream-function field would be obtained using the grid point winds generated by the new analysis procedure. Evidently, this is not always the case.

This Faye forecast was originally selected because it was particularly poor at 48 and 72 hours. The southerly flow to the west of the high (see Figure 7) became southwesterly and strengthened causing the high to move south and east. The SANBAR model was not able to simulate these effects. The high was forecast to retrogress westward in both SANBAR runs. The forecasts were unable to produce the acceleration which was observed in the actual track. The failure of SANBAR to show recurvature and acceleration northeast was due in part to its failure to put the storm in the proper location at 48 hours. Although the new analysis procedure was expected to improve the initial analysis, it could not be expected to correct the primary problem in this forecast, that of baroclinic effects.

Six of the selected forecasts were affected by the loss of the stream-function minimum. To obtain an estimate of the significance of this problem, the mean position errors were

recalculated after the elimination of all position errors for any forecast times at which the stream-function minimum was lost in one forecast and retained in the other. The results are shown in Table 13. A comparison of the differences observed in the mean position errors of the original sample of selected forecasts (see Tables 6 and 7) and those of this smaller sample indicate a reduction in the position errors for the smaller sample, except at 24 hours, with the most substantial reductions occurring at 36 and 72 hours. It appears that the variation in the retention of the stream-function minimum might have accounted for one-quarter to one-third of the increase in the position errors which occurred in the rerun forecasts.

This problem would not have occurred if the vorticity maximum alone had been used in determining the forecast positions. The use of only the vorticity maximum seems reasonable since the physical basis for the model is conservation of absolute vorticity and since the stream-function minimum is frequently lost in the forecasts as previously explained. Sanders and Gordon (1976) found no improvement of forecast positions using the vorticity maximum alone, but recommended its use because it makes better physical sense.

Analysis Poleward of 45°N

Wind analysis poleward of 45°N latitude is extremely

TABLE 13. Mean position errors (n mi) for selected cases excluding cases in which the stream-function minimum was lost in one forecast and retained in the other.

OPERATIONAL FORECASTS				
	<u>24 hr</u>	<u>36 hr</u>	<u>48 hr</u>	<u>72 hr*</u>
Mean	108 (21)	212 (19)	286 (17)	558 (9)
RERUN FORECASTS				
	<u>24 hr</u>	<u>36 hr</u>	<u>48 hr</u>	<u>72 hr</u>
Mean	115 (21)	213 (19)	302 (17)	584 (9)
Change from the operational	+7	+1	+16	+26

*The 72 hour position errors are much larger than those shown in Tables 6 and 7 because more good forecasts than bad forecasts were eliminated.

() Number in sample

difficult, due to the paucity of data in this region. In several of the selected forecasts, substantial differences occurred in the initial stream-function patterns produced by the two analysis procedures in the extreme northeast portion of the SANBAR grid. In the operational forecasts, three bogus winds located in the North Atlantic at bogus points 1, 2, and 3 (see Figure 1) were used in the Eddy statistical analysis to determine grid point winds in this region. All information which was available at NHC at the initial time was used to obtain an estimate of the winds at these bogus points. In the rerun forecasts, the Eddy analysis continued to be performed in this region, because the ATOLL and 200-mb analyses extend only to 45°N. Since the grid point winds in other oceanic portions of the grid were obtained without reference to the bogus winds, bogus points 1, 2, and 3 were also eliminated for the sake of simplicity, time, and convenience. Thus the Eddy analysis was carried out north of 45°N latitude without the aid of the bogus point winds. This resulted in a number of odd initial stream-function patterns in this region. When the analysis is performed in an area in which few data are available, the winds tend to take on the value of the latitudinal mean, in this case, direct westerly flow. This was observed in several of the rerun forecasts, but was most obvious for and had the most significant effect upon the Amy forecasts since this storm was located farther north

than the other storms when forecasts were made. The result was a deterioration of the SANBAR forecasts.

The difference in the wind analyses produced with and without the use of the three northernmost bogus points, and the resulting forecast differences, can be seen in the selected case of Amy, beginning at 0000GMT on the 1st of July. Amy originated as a tropical depression off the east coast of Florida in late June and reached tropical storm strength on the first of July while located near the outer banks of North Carolina. Although the storm occasionally approached hurricane intensity, it remained predominantly subtropical in nature. A trough which developed over northeastern Canada on July 3rd caused Amy to accelerate rapidly northeastward; on the 4th of July, while southeast of Newfoundland, Amy lost all its tropical characteristics.

The best-track and the operational and rerun forecast tracks for Amy beginning at 0000GMT on July 1st are shown in Figure 9. Position errors for the two SANBAR forecasts are given in the table below. This case was selected for rerun

TABLE 14. Position errors (n mi) for SANBAR forecasts for Amy, July 1, 0000GMT.

	<u>00 hr</u>	<u>12 hr</u>	<u>24 hr</u>	<u>36 hr</u>	<u>48 hr</u>	<u>72 hr</u>
Operational	15	46	123	123	202	645
Rerun	15	61	138	170	259	715
Change from the operational						
	0	+15	+15	+47	+57	+70

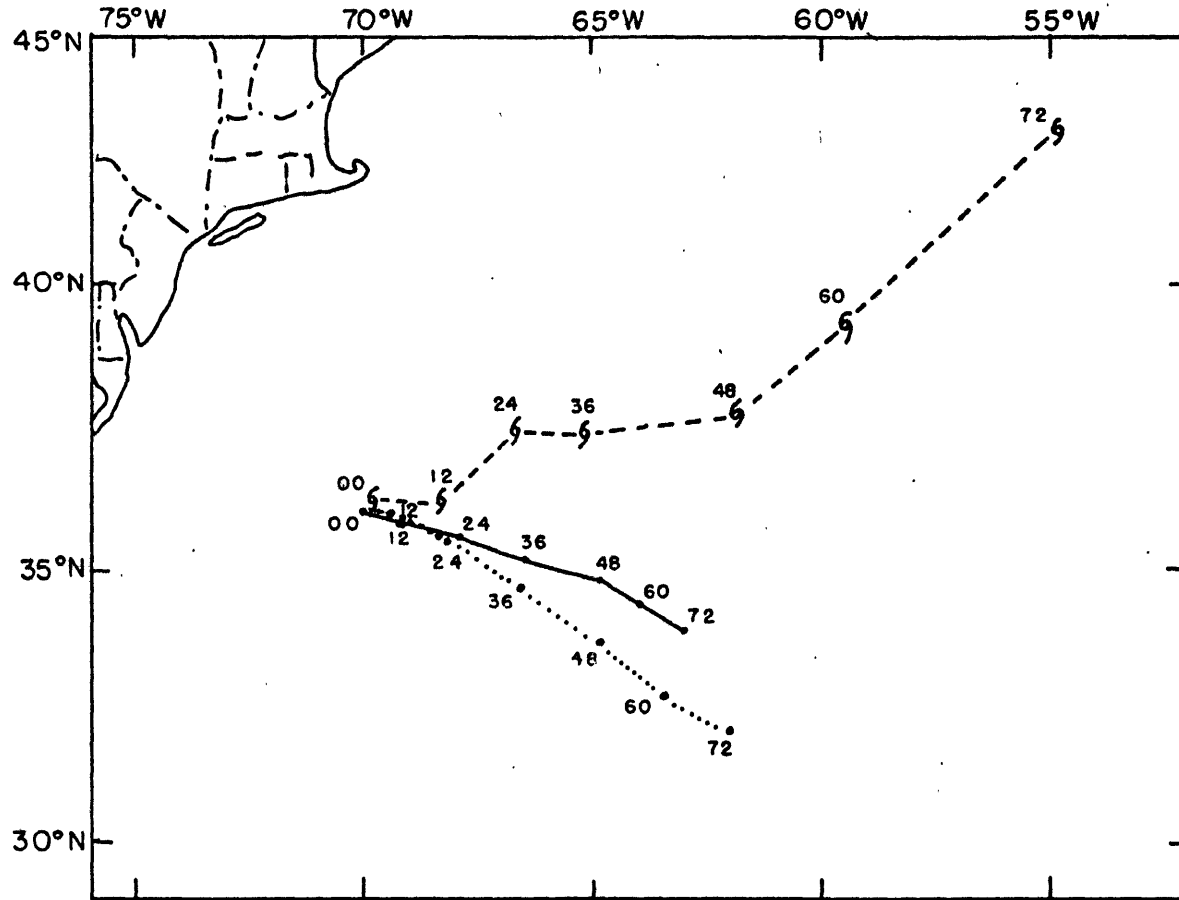


Figure 9. Tracks of Amy, July 1, 0000GMT. Notation the same as Figure 6.

because of the large 72-hour position error observed in the operational forecast. However, the rerun forecast which was made using the new analysis procedure produced an even greater position error at 72 hours, as well as at all other forecast ranges.

While the storm moved generally toward the northeast, both the operational and rerun forecasts predicted an overall northwesterly movement, with the rerun track showing displacement farther to the right of the observed track than the operational track. All forecast speeds were slower than the observed speeds, although speeds predicted in the rerun forecast were greater than those predicted in the operational run. The initial storm direction and speed (toward 90° at 3 knots), which was used in both forecasts, was probably responsible for the slowness predicted at early times.

The initial stream-function fields for the two SANBAR forecasts are shown in Figure 10. The patterns are very similar over most of the grid, and the center of the high pressure system in which the storm is embedded is at approximately the same location in both analyses. Over oceanic regions in the northeast corner of the grid, substantial differences in the two stream-function analyses are apparent. The stream-function field for the operational forecast shows a trough in this region with southwesterly flow from 55° W longitude eastward to the edge of the SANBAR grid. The stream-function

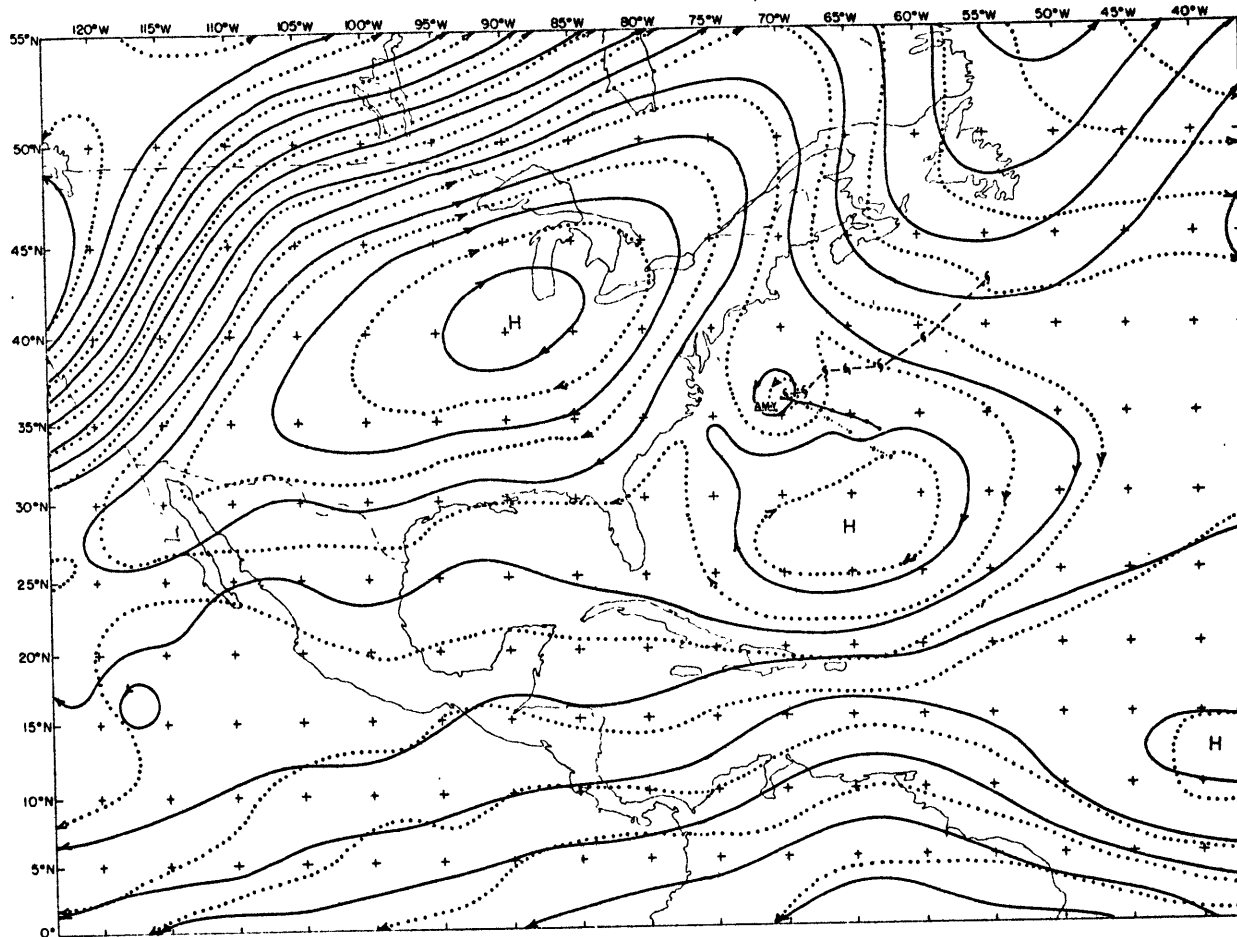


Figure 10. Initial analyses of large-scale flow pattern, July 1, 0000GMT, for the operational and rerun SANBAR forecasts. Notation the same as Figure 7.

analysis for the rerun shows westerly and northwesterly flow in this same region.

Mean bogus winds used in the operational analysis and mean grid point winds used in the rerun analysis are shown in Figure 11. The winds at bogus points 1, 2, and 3 show strong southwesterly flow. Northwesterly winds are indicated at grid points near bogus point 1, while west-northwesterly and westerly grid point winds are observed near bogus points 2 and 3. The rerun analysis in this area seems unrealistic. Just south of 45°N , winds are southerly; while just north of 45°N , they abruptly become westerly.

In the operational forecast, the high retrogressed westward and the storm was predicted to move toward the southeast along the edge of the high. In the rerun forecast, the stream-function analysis in the northeastern portion of the grid produced height falls east of the high. The high retrogressed even farther westward, causing the rerun track to be even farther to the right of the observed track than had been predicted in the operational run. Neither forecast was able to move the high eastward and to predict the development and intensification of the trough in which the storm became embedded.

It is difficult to hypothesize whether the rerun would have shown improvement over the operational forecast if the winds at bogus points 1, 2, and 3 had been used. However,

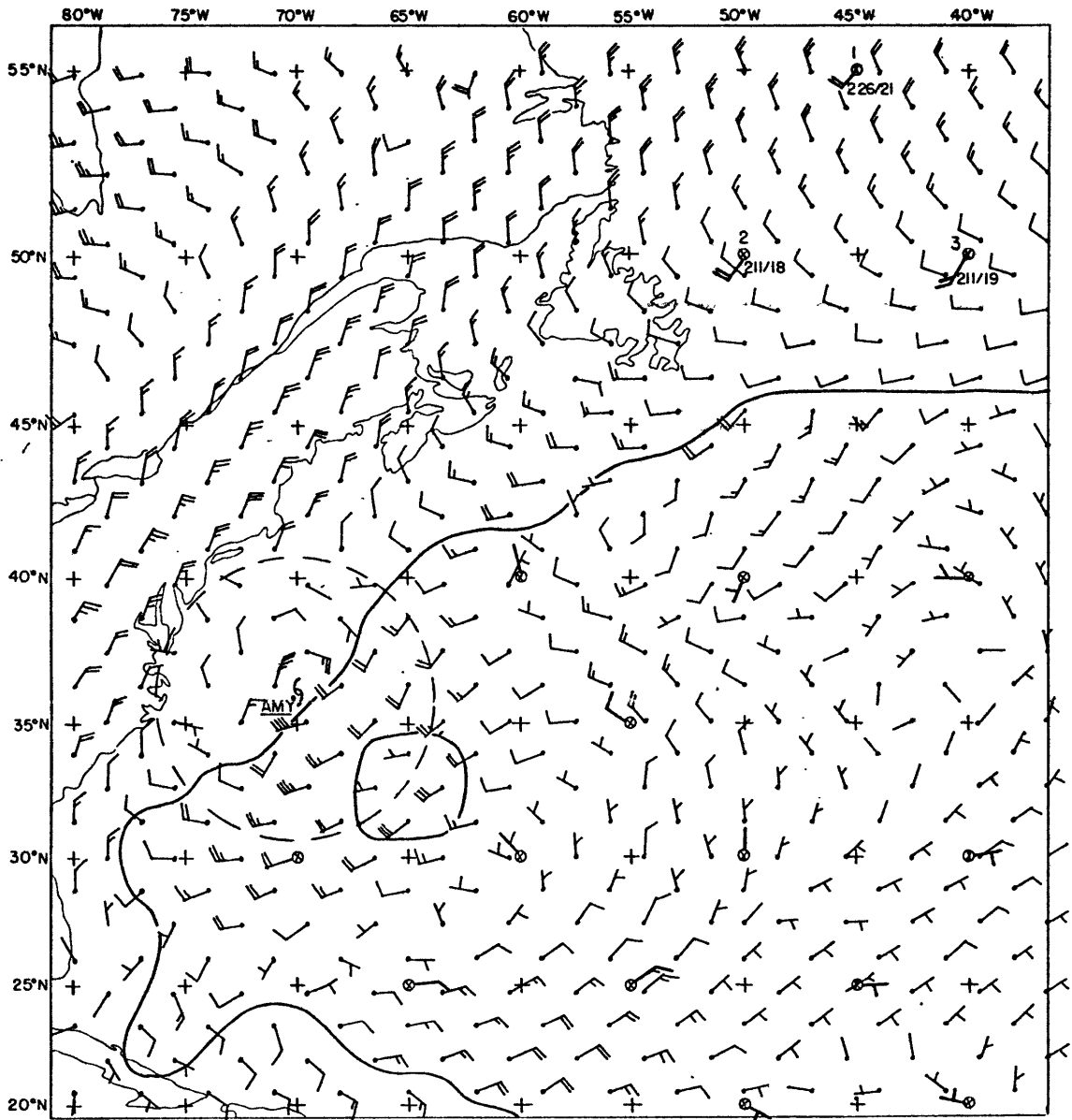


Figure 11. Bogus winds and SANBAR grid point winds for the forecasts beginning at 0000GMT on July 1. Notation the same as Figure 8.

a better initial analysis should lead to a better forecast, and the stream-function pattern produced without these bogus winds was probably not an accurate representation of the mean tropospheric flow. Consideration should be given to producing a more realistic analysis in the northeast portion of the grid, either by a return to the bogus point estimation or by some more convenient method. However, only a limited number of forecasts will be affected by the analysis in this area, since any storm this far northeast is generally outside of the area of NHC responsibility.

Excessive Weighting of 200-mb Level Winds

Although winds within the influence distance of the storm are discarded in the analysis, there is evidence of strong westerly outflow from the storm beyond the area of influence in some of the SANBAR forecasts. This outflow generally occurs only in a very shallow layer, often near the 200-mb level. Upper-level winds which are affected by this outflow will not be representative of the basic flow. When these non-representative 200-mb winds are combined with the ATOLL level winds in the regression equations, the resulting mean winds will not give an accurate representation of the large-scale current assumed to steer the storm. The occurrence of the outflow and its effects are most apparent when the westerly winds are embedded in an area of generally

easterly current.

Evidence for this westerly outflow appeared in several of the selected forecasts, particularly those made for Faye and Gladys while these storms were traveling westward from the middle Atlantic and when recurvature was just beginning. It appeared to be less of a problem in the operational forecasts than in the reruns because of the particular analysis procedure utilized in oceanic areas. The westerly outflow went undetected in the wind analysis for the operational runs unless a bogus point was located within the region of outflow. Because of the small number and dispersion of the bogus points, this did not often occur. When a bogus wind was affected, only a small number of grid point winds located nearby reflected this westerly flow. In the new analysis method used in the reruns, all the grid points located in the outflow area were adversely affected.

The storm outflow and its effects on the SANBAR forecasts can be seen in an examination of the forecast for Gladys beginning on September 26th at 1200GMT. Gladys, like Faye, developed from a depression which originated off the west coast of Africa. The storm followed a path parallel to Faye's track although generally south and west of it. Gladys was designated a hurricane while still located in the middle Atlantic, before any ship reports or reconnaissance aircraft information became available. Hurricane winds were first re-

ported late on the 25th of September. On the 28th, the storm began to intensify until the central pressure reached 975 mb. This pressure was maintained until recurvature began on the first of October. Gladys then deepened rapidly and accelerated toward the northeast. The storm weakened only slightly before crossing the North Atlantic shipping lanes.

The best-track and SANBAR forecast tracks for Gladys beginning September 26th at 1200GMT are shown in Figure 12. Position errors are given in the table below. This case was

TABLE 15. Position errors (n mi) for the SANBAR forecasts for Gladys, September 26, 1200GMT.

	<u>00 hr</u>	<u>12 hr</u>	<u>24 hr</u>	<u>36 hr</u>	<u>48 hr</u>	<u>72 hr</u>
Operational	6	35	79	126	113	222
Rerun	6	41	108	166	181	377
Change from the operational	0	+6	+29	+40	+68	+155

selected because of the relatively small 72-hour position error. Position errors for the rerun forecasts were greater at all forecast ranges than those for the operational run; The difference increased with time. Both the operational run and the rerun forecast showed left biases; however, the rerun track was farther to the left of the observed track than the operational SANBAR track. The loss of the stream-function minimum at 72 hours in the original run reduced the

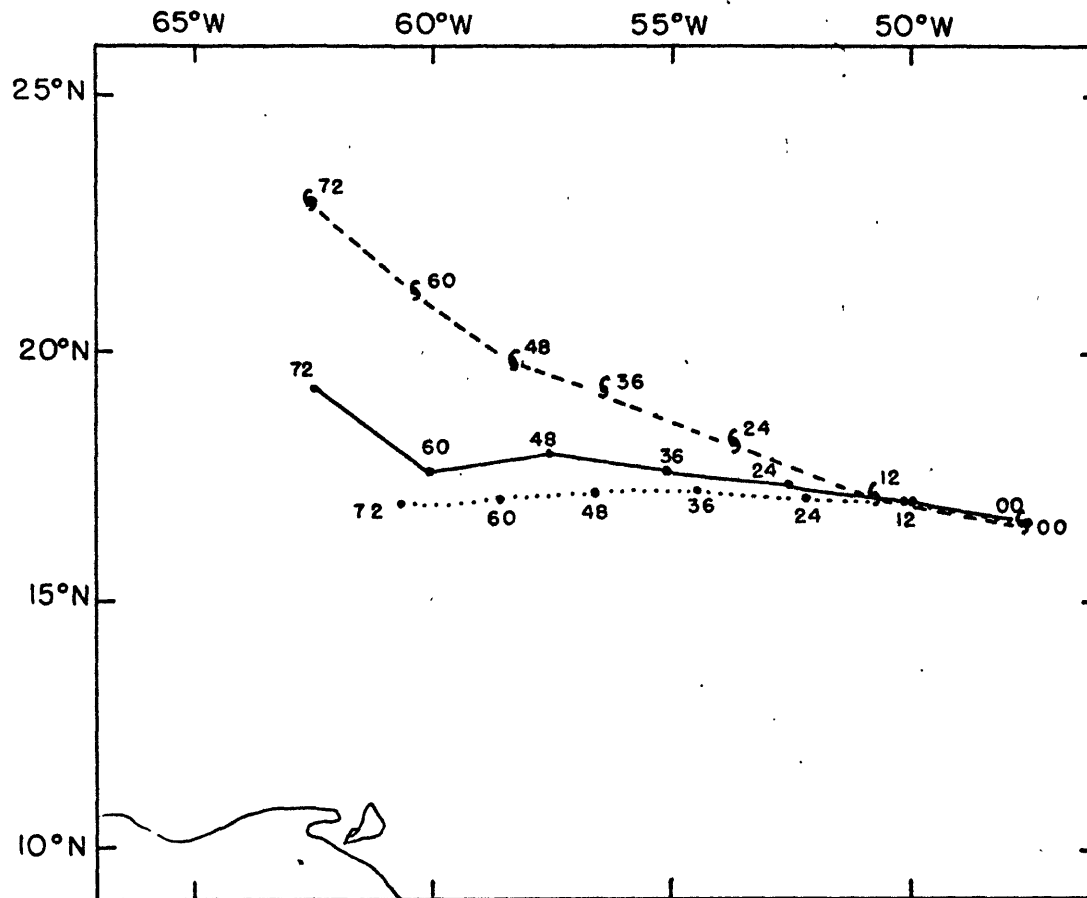


Figure 12. Tracks of Gladys, September 26, 1200GMT. Notation the same as Figure 6.

position error at that time. The rerun forecast did not receive this benefit. Although both forecasts moved the storm too slowly, the rerun forecast showed the greater slow bias.

The initial stream-function analyses for the operational and rerun SANBAR forecasts are shown in Figure 13. The stream-function patterns are quite similar, except in the extreme southeast portion of the grid and particularly east of Gladys. In this region, the rerun analysis indicates much weaker flow than indicated by the operational analysis. An examination of grid point winds used in the rerun and bogus winds used in the original run (see Figure 14) reveals the reason for this difference. In the bogus winds, there is very little evidence of westerly storm outflow. Easterly flow is indicated at bogus points 15 and 19 located northwest and west of Gladys. Northeasterly flow at bogus point 29, southeast of the storm, becomes east-southeasterly flow at bogus point 28, south of the storm.

On the other hand, grid point wind values used in the rerun forecast show strong evidence of the outflow.¹ Several northwesterly winds appear northeast of the storm between 20°N and 25°N. Westerly winds are also observed between 10°N

¹Only every other grid point wind was computed. Therefore the grid point winds shown here represent only half of those used in the model.

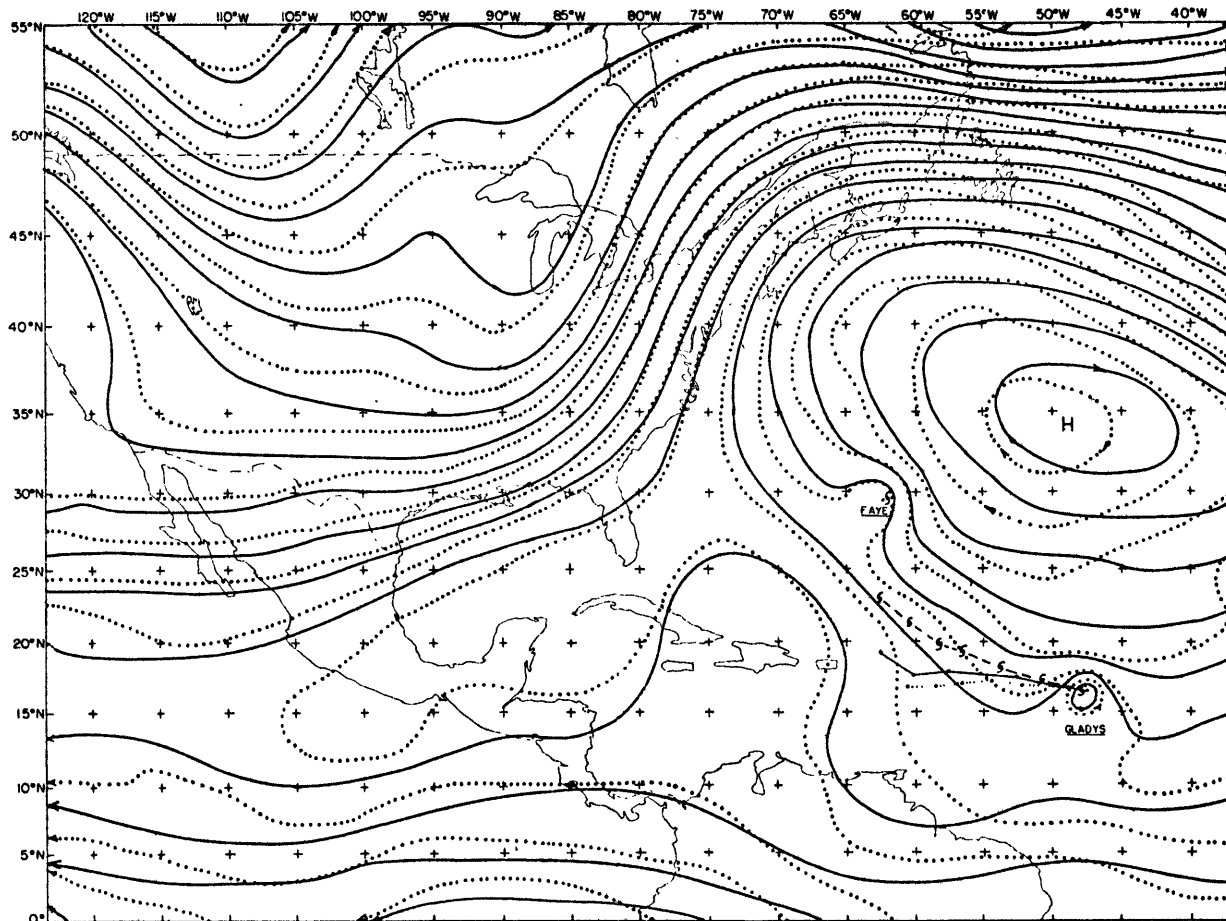


Figure 13. Initial analyses of large-scale flow pattern, September 26, 1200GMT, for the operational and rerun SANBAR forecasts. Notation the same as Figure 7.

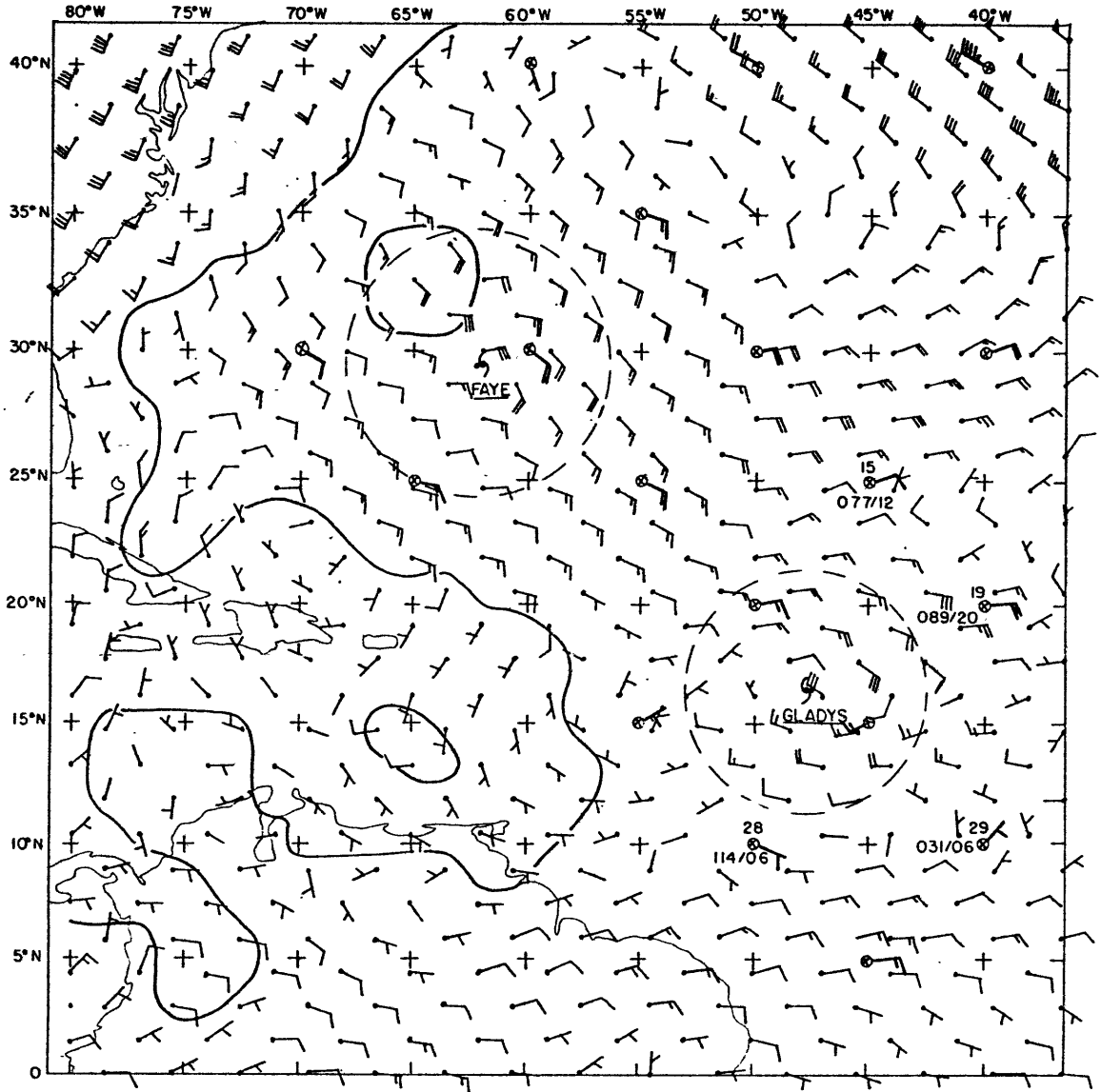


Figure 14. Bogus winds and SANBAR grid point winds for the forecasts beginning at 1200GMT on September 26. Notation the same as Figure 8.

and 18°N west and southwest of the storm. Although very little data was available east of the storm, the wind data used at NHC in the correction of the guess fields showed moderate easterly flow at the ATOLL level and strong westerly flow at the 200-mb level. Evidently, too much weight was given to the 200-mb level winds in the regression equations. The resulting mean winds were not representative of the mean tropospheric flow in this area.

This difficulty raises the question of using three levels rather than two to determine the mean tropospheric flow. Many of the winds used in the ATOLL and 200-mb analyses are wind estimates based on cloud-motion vectors derived from geosynchronous satellites. The motion of the low-level and high-level clouds are assumed to represent winds at 3000 to 5000 feet and 30,000 feet, respectively (Hubert and Whitney, 1971). Occasionally middle-level clouds are identified and assigned to the 500-mb level. Adams and Sanders (1975) developed regression equations based on three levels and found less regression analysis was necessary when three levels were used. Unless more data for the 500-mb level becomes available, however, the model must continue to rely on the ATOLL and 200-mb analyses only.

Errors in the Stream-function and Vorticity Fields Within the Area Influenced by the Storm

The distances between the operational and rerun fore-

cast positions were computed for the selected cases. The means of the distances are shown in Table 16. The greatest differences between the two SANBAR forecasts for every forecast range occurred in one case, Gladys beginning at 1200GMT on the 28th of September. The differences, 46, 88, 130, 169, and 252 nautical miles for 12, 24, 36, 48, and 72 hours respectively, were much greater than the total sample means shown in the table. This Gladys forecast gives an indication of the maximum difference in forecast tracks which can be expected when the two different methods of analysis are used over oceanic regions.

The best-track and forecast tracks for Gladys, September 28, 1200GMT are shown in Figure 15. Although the two forecast tracks were very different, the position errors generated were approximately the same (see Table 17). Slightly

TABLE 17. Position errors (n mi) for SANBAR forecasts for Gladys, September 28, 1200GMT.

	<u>00 hr</u>	<u>12 hr</u>	<u>24 hr</u>	<u>36 hr</u>	<u>48 hr</u>	<u>72 hr</u>
Operational	8	72	157	189	224	292
Rerun	8	83	166	211	250	331
Change from the operational	0	+11	+9	+22	+26	+49

greater errors were observed at all forecast ranges in the rerun. The new analysis procedure greatly improved the track direction, but reduced the storm speed producing an even slower bias in the rerun forecast than observed in the

TABLE 16. Mean distances (n mi) between operational and rerun SANBAR forecast positions for the selected cases.

	<u>00 hr</u>	<u>12 hr</u>	<u>24 hr</u>	<u>36 hr</u>	<u>48 hr</u>	<u>72 hr</u>
Amy	0 (4)	9 (4)	29 (4)	44 (3)	72 (2)	125 (2)
Caroline	0 (2)	0 (2)	7 (2)	24 (1)	53 (1)	—
Doris	0 (3)	2 (3)	8 (3)	18 (3)	33 (3)	69 (2)
Eloise	0 (3)	4 (3)	9 (3)	22 (3)	21 (3)	43 (3)
Faye	0 (4)	7 (4)	23 (4)	39 (3)	60 (3)	148 (2)
Gladys	0 (8)	12 (8)	28 (8)	46 (8)	69 (7)	137 (5)
<u>Mean</u>	0 (24)	7 (24)	21 (24)	36 (21)	54 (19)	107 (14)

()Number in sample

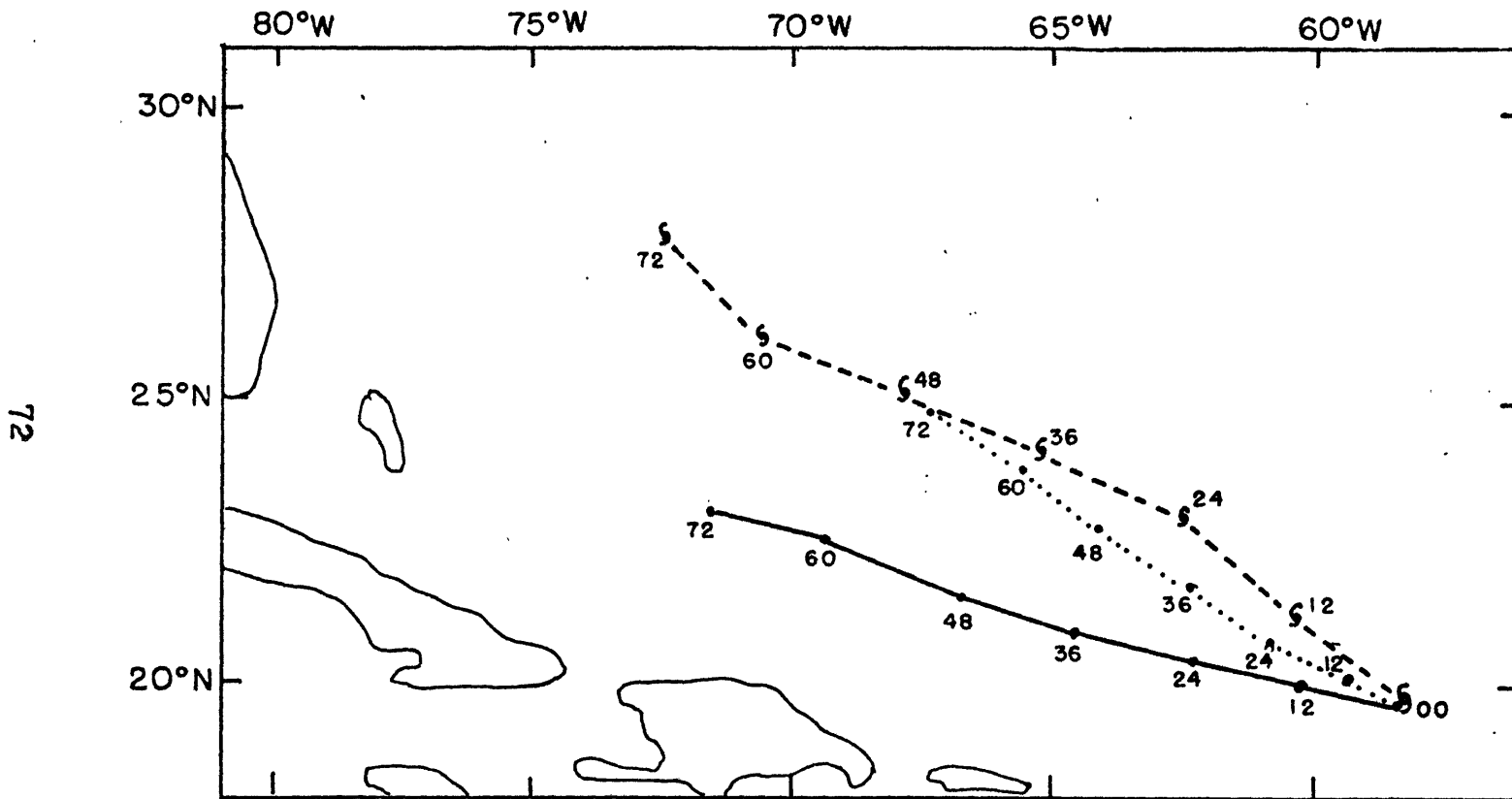


Figure 15. Tracks of Gladys, September 28, 1200GMT. Notation the same as Figure 6.

operational run. The initial storm direction and speed for both runs was toward 270° at 10 knots. Usually this direction and speed are returned in the first 12 hours. However, this did not occur in this Gladys forecast. In the operational run, the storm moved toward 285° at 10 knots in the first 12 hours, while the rerun showed movement toward 295° at 6 knots. At the same time, the best-track showed the storm moving toward 310° at 11.5 knots.

The improved directions and slower speeds of the rerun forecast are reflected in the initial stream-function analysis shown in Figure 16. The mean tropospheric flow as indicated by the stream-function pattern is southeasterly near the storm in the rerun, but more directly from the east in the operational analysis. This weaker flow is also revealed in the wind information shown in Figure 17. The 18-knot wind at bogus point 23 was stronger than most of the surrounding grid point winds used in the rerun. Grid point winds west and south of bogus point 29 and west and north of bogus point 18 were also slower than the bogus winds of 12 and 8 knots.

In examining the SANBAR forecasts for this Gladys case, a discrepancy in the vorticity fields within the influence distance was discovered. Because the storm parameters were taken to be the same in both the operational and revised forecasts, the values of vorticity at the grid points within this area should have been identical. However, vorticity differ-

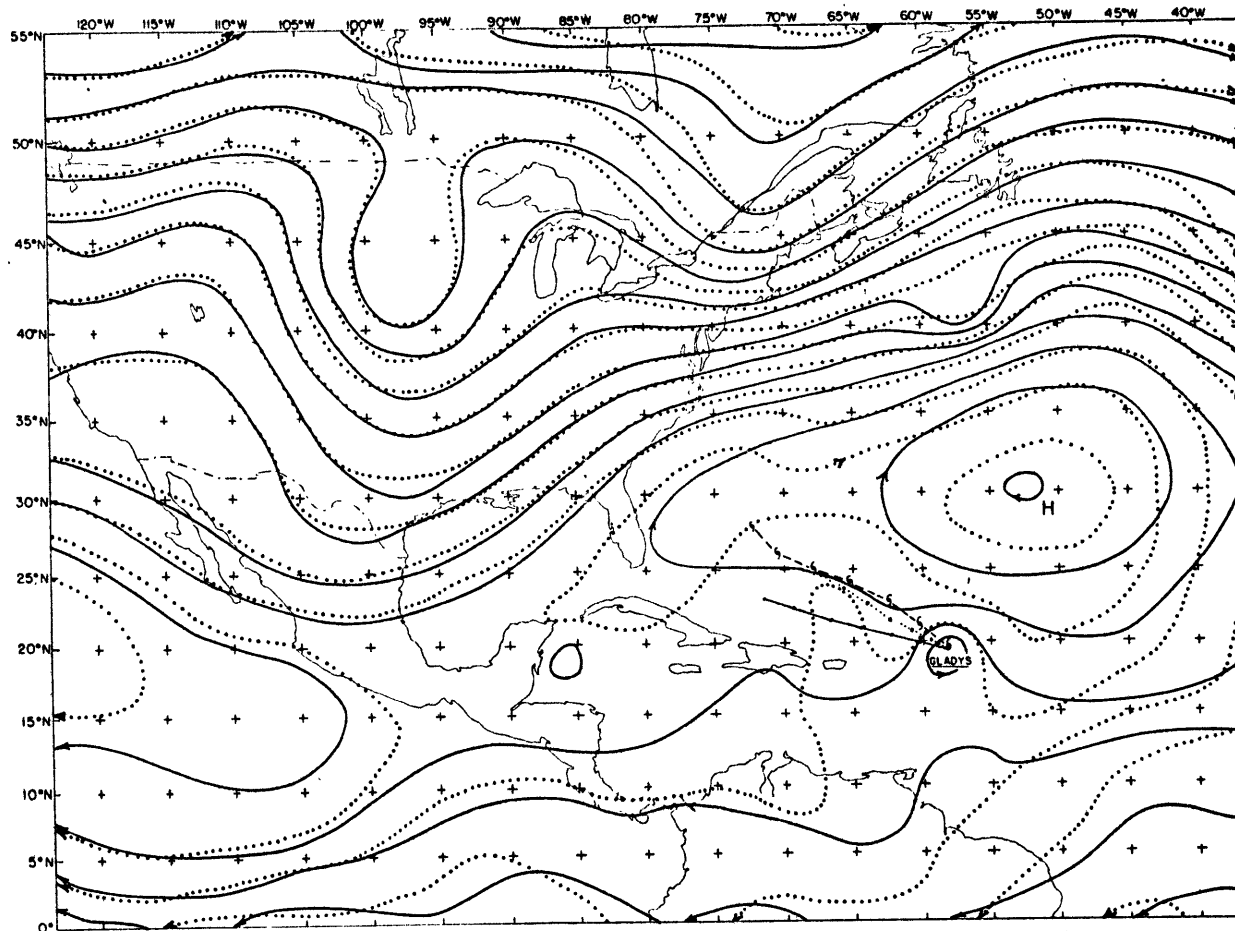


Figure 16. Initial analyses of large-scale flow pattern, September 28 , 1200GMT for the operational and rerun SANBAR forecasts. Notation the same as Figure 7.

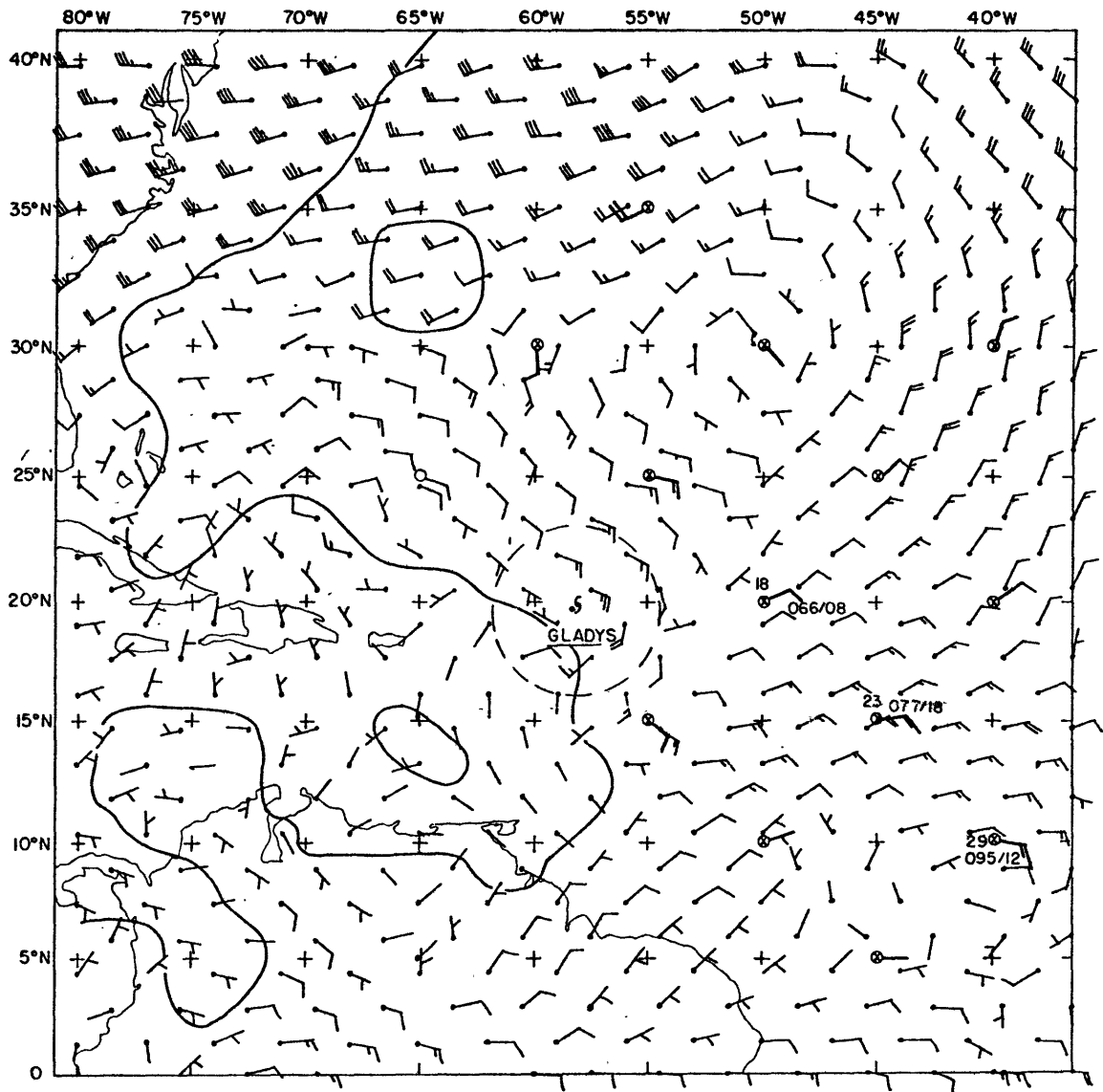


Figure 17. Bogus winds and SANBAR grid point winds for the forecasts beginning at 1200GMT on September 28. Notation the same as Figure 8.

ences were observed in these forecasts. Comparison of the vorticity fields for the other selected cases revealed the same peculiarity in six other instances. After closer examination, it was learned that the proper storm wind profile had not been used in these particular reruns; this led to incorrect values of vorticity at the grid points within the influence distance of the storm. Although these incorrect vorticity values had little effect on the forecast tracks, another programming error was detected which could have been at least partially responsible for the increased slow bias observed in the revised forecasts.

In searching for causes of the slow bias in the SANBAR forecasts from the 1971 hurricane season, Sanders et al. (1975) found that the strength of the steering flow was too weak. This strength is given by $\Delta\psi/2R$, where R is the maximum influence radius, and $\Delta\psi$ is the difference of stream-function values at the two ends of a line segment normal to the prescribed storm direction, centered on the storm. The relaxation procedure for obtaining the initial stream-function from the calculated vorticity was failing to reproduce the correct steering speeds in the vicinity of the storm. To correct this problem, the vorticity and stream-function fields were precalculated at all grid points within the influence distance of the storm. Revised forecasts based on this FAST SANBAR model showed a decrease in the slow bias.

Although FAST SANBAR is the model currently used operationally at NHC, this version of SANBAR was evidently not used in the Gladys forecast of September 28th, 1200GMT. Estimates of the strength of the steering current were made using the formulation mentioned earlier. A basic flow of approximately 7 knots was indicated by the rerun stream-function field, while one of approximately 12 knots was indicated by the operational analysis. As shown in Table 5, the initial storm speed was given as 10 knots, which was much greater than the estimate determined from the large-scale flow for the revised forecast. This also appeared to be the case in the other six forecasts where mistaken vorticities were observed.

The mean position, direction, and speed errors were recalculated after the elimination of these 7 erroneous cases. The results are shown in Table 18. Also shown are the differences between the mean errors for the operational and rerun forecasts for both this sample and for the entire set of selected cases. Although the rerun mean position errors were not significantly different from the operational means, larger errors were still observed in the revised forecasts at 24, 36, 48, and 72 hours. Position errors were slightly improved at 12 and 24 hours in the smaller sample, but were worse at 36 and 72 hours. The differences in the algebraic means of the direction errors were greater in the

TABLE 18. Mean errors for the operational and rerun selected cases excluding forecasts with incorrect vorticity values.

MEAN POSITION ERRORS (n mi)

	<u>00 hr</u>	<u>12 hr</u>	<u>24 hr</u>	<u>36 hr</u>	<u>48 hr</u>	<u>72 hr</u>
Operational	12	46	97	198	317	510
Rerun	12	46	101	203	336	558
Change from the operational	0	0	+4	+5	+19	+48
Change from the operational in the original sample	0	+2	+6	+3	+19	+37

MEAN SPEED ERRORS (n mi)

Algebraic Means

Mean Magnitudes

	<u>00-24hr</u>	<u>24-48hr</u>	<u>48-72hr</u>	<u>00-24hr</u>	<u>24-48hr</u>	<u>48-72hr</u>
Operational	-35	-131	-298	61	150	298
Rerun	-38	-152	-319	61	162	319
Change from the operational	+3	+21	+21	0	+12	+21
Change from the operational in the original sample	+10	+14	+20	+6	+6	+20

MEAN DIRECTION ERRORS (n mi)

Algebraic means

Mean magnitudes

	<u>00-24hr</u>	<u>24-48hr</u>	<u>48-72hr</u>	<u>00-24hr</u>	<u>24-48hr</u>	<u>48-72hr</u>
Operational	-24	-54	-74	42	89	90
Rerun	-24	-37	-30	45	95	75
Change from the operational	0	-17	-44	+3	+6	-15
Change from the operational in the original sample	-10	-28	-47	-2	+20	-11

smaller sample, although the differences in the mean magnitudes was less during the last two 24-hour periods. Differences in mean speed errors increased during some intervals and decreased during others. It appears that the programming errors might have been responsible for a portion of the slow bias at early times, but was probably not the cause of the slow speeds at later times.

The revised forecasts are continuing to be examined to determine if FAST SANBAR might not have been used in other selected forecasts. If it was used in the remaining forecasts, the cause of the slow bias must lie elsewhere.

CONCLUSIONS

A new analysis procedure which makes more and better use of the available data and which makes no reference to the bogus winds used in the operational SANBAR model was introduced for use in oceanic regions. Selected forecasts were rerun using this revised technique, and the results were compared with the operational forecasts. Overall, the new method of analysis improved track directions, but produced a greater slow bias than observed in the original runs.

Elimination of bogus winds poleward of 45°N latitude led to poor initial analyses in the northeast portion of the SANBAR grid in some of the reruns. A convenient procedure

should be developed to obtain a better analysis in this area.

In cases where strong westerly outflow from the storm was observed, the initial analysis east of the storm, which was produced using the revised procedure, was not representative of the large-scale flow. This resulted in the deterioration of some of the SANBAR forecasts. If more satellite data for the 500-mb level becomes available, the use of three levels, rather than two, in the regression analysis might prove advantageous.

In several of the selected forecasts, errors were made in computing the vorticity and stream-function fields within the influence distance of the storm. FAST SANBAR was not used in these forecasts. The revised forecasts are being examined to determine if FAST SANBAR was not used in any of the other reruns. If this was the case, the extra element of slowness observed when using the new method of analysis might be eliminated. In that event, the new technique might prove to reduce speed errors as well as direction errors in the SANBAR forecasts. If FAST SANBAR was used, one will have to look elsewhere for the cause of the greater slow bias.

At the present time, it appears that the revised analysis procedure is no better, and no worse, than the current analysis technique used operationally at NHC.

REFERENCES

- Adams, A.L., and F. Sanders, 1975: Application of satellite cloud motion vectors to hurricane track prediction. Massachusetts Institute of Technology. Scientific Report No.1, AFCRL Contract F19628-75-C-0059. Report Number AFCRL-TR-75-0635. 57pp.
- Ahn, C.S., 1967: Numerical prediction of hurricane movement. M.S. Thesis, Massachusetts Institute of Technology.
- Cooley, D.S., 1974: A description of the Flattery global analysis method--No.1. Technical Procedures Bulletin No.105. Weather Analysis and Prediction Division, NMC.
- Cressman, G.P., 1959: An operational objective analysis system. Mon. Wea. Rev., 87, 367-374.
- Eddy, A., 1967: The statistical objective analysis of scalar data fields. J. Appl. Meteor., 6, 597-609.
- Hebert, P.J., 1976: Atlantic hurricane season of 1975. Mon. Wea. Rev., 104, 453-465.
- Hubert, L.F., and L.F. Whitney, Jr., 1971: Wind estimation from geostationary-satellite pictures. Mon. Wea. Rev., 99, 665-672.
- King, G.W., 1966: On the numerical prediction of hurricane trajectories. M.S. Thesis, Massachusetts Institute of Technology.
- Pike, A.C., 1972a: Improved barotropic hurricane track prediction by adjustment of the initial wind field. NOAA Tech. Memo. NWS SR-66.
- _____, 1972b: Personal communication.
- _____, 1975: Personal communication.

REFERENCES (CONT'D)

- Sanders, F., and N.J.Gordon, 1976: A study of forecast errors in a barotropic operational model for predicting paths of tropical storms. Massachusetts Institute of Technology. Scientific Report No.2. 56pp. in press.
- _____, A.C.Pike and J.P.Gaertner, 1975: A barotropic model for operational prediction of tracks of tropical storms. J. Appl. Meteor., 14, 265-280.
- Williams, F.R., 1972: Application of the SANBAR hurricane track forecast model. M.S. Thesis, Massachusetts Institute of Technology.
- Wise, C.W., and R.H.Simpson, 1971: The tropical analysis program of the National Hurricane Center. Weatherwise, 24, 164-173.

APPENDIX A

Elliptical Scanning Procedure

The elliptical scanning technique, used to obtain grid point winds at the ATOLL and 200-mb levels, involves the application of corrections to a "first guess" field. The analysis procedure is similar to that developed by Cressman, except that an elliptical area, rather than a circular area, is used in the scanning process. The ellipse is oriented along the wind direction, thus giving more weight to the data upstream and downstream than to the data on either side.

At the grid point to be examined, an interpolated value of the wind is determined from the guess field. An elliptical area is centered on the grid point, and a comparison is made between each data point within the ellipse and the interpolated value. The difference between the interpolated and the wind at each data point is multiplied by a weighting factor. The correction to the guess field is obtained by averaging the products of the weighted differences. This averaging results in a smoothing within the elliptical area. Once this procedure has been performed at each grid point, the process is repeated using a smaller elliptical area. A series of scans is made to allow for the analysis of various scales. The largest ellipse permits the correction of the largest-scale errors in the first guess field, and the smallest ellipse limits the scale analyzed. Further smoothing is re-

quired to eliminate discontinuities which arise when the first guess is poor.

APPENDIX B

Eddy Statistical Analysis

The Eddy analysis procedure provides the multiple regression equations used for computing the mean winds at all SANBAR grid points from the observed values at nearby bogus points and rawinsonde stations. This procedure also provides regression equations for any missing stations which are on the station list required by the model. The Eddy analysis is based on the correlation of the observed departures of the zonal and meridional wind components from the latitudinal means as a function of the distance between observations. Figure B1 shows two correlation functions derived from different sets of data (Sanders et al., 1975). The curves have been smoothed and extended parabolically to zero. The sample of data used in the derivation of the correlation function was large and included observations over a long period of time and data from the Gulf of Mexico, the Caribbean Sea, the eastern Pacific Ocean, North America, and the western and central portions of the Atlantic Ocean. Spurious observations were corrected or eliminated from the data, and any observations which were influenced by a tropical storm were also eliminated. In deriving the curves, the statistics of the

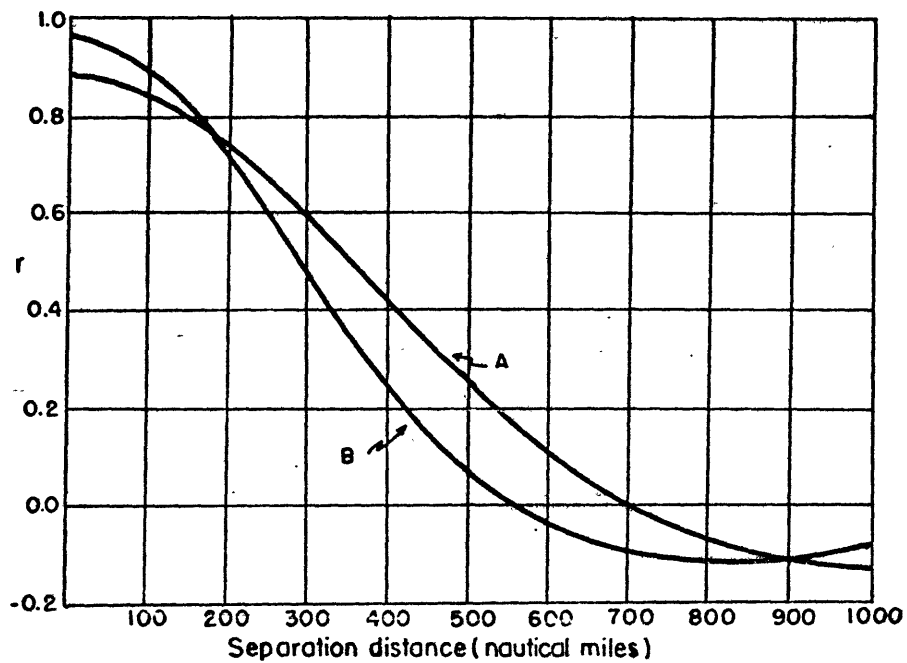


Figure B1. Correlation as a function of separation distance for departures of vertically-averaged wind from synoptic zonal average value. Curve A was derived from a sample of 1799 soundings on selected hurricane days in September of 1960, 1961, and 1965 and October of 1963, 1965, and 1967. Curve B was derived from a sample of 1713 soundings from September 6 through September 13 of 1971. (From Sanders et al., 1975).

wind data were assumed to be isotropic, homogeneous, and stationary.

All observations, either at rawinsonde stations or at bogus points, within the zero-correlation distance given by the correlation function are utilized in the derivation of the regression equation for each SANBAR grid point. A multiple linear regression equation is obtained by stepwise screening regression based upon the correlation coefficient associated with the distance from the observations to the grid point and the distance between observation. Observations are continually added until the marginal increase in the unexplained variance is less than a tenth of one percent.

The zonal and meridional components of the mean tropospheric wind at the SANBAR grid points which result from this Eddy analysis are used as input to the SANBAR hurricane track forecast program to obtain initial stream-function and vorticity fields over the SANBAR grid.